Urban Climate 23 (2018) 309–329

Contents lists available at ScienceDirect

Urban Climate

journal homepage: http://www.elsevier.com/locate/uclim

The cooling effect of irrigation on urban microclimate during heatwave conditions

Ashley M. Broadbent[a, b, c, *], Andrew M. Coutts[b, c], Nigel J. Tapper[b, c], Matthias Demuzere[d]

[a] Arizona State University, School of Geographical Sciences and Urban Planning, Tempe, AZ, USA
[b] Monash University, School of Earth Atmosphere and Environment, Melbourne, Australia
[c] Cooperative Research Centre (CRC) for Water Sensitive Cities, Melbourne, Australia
[d] UGhent, Department of Forest and Water Management, Ghent, Belgium

ARTICLE INFO

Article history:
Received 2 June 2016
Received in revised form 31 March 2017
Accepted 11 May 2017
Available online xxxx

Keywords:
Urban microclimate
Water sensitive urban design
Integrated urban water management
Urban heat mitigation
Irrigation
Urban water cycle
TEB
SURFEX

ABSTRACT

The emergence of integrated urban water management (IUWM), provides a unique opportunity for passive evaporative cooling of urban environments. This study investigates the potential of purposefully managed irrigation for cooling benefits in a suburb of Adelaide, Australia, where IUWM is widely adopted. SURFEX was used to simulate heatwave conditions across a suburban environment. Results from two simulation periods are presented: model validation period and a heatwave case study. Model validation suggests SURFEX can broadly capture the average intra-suburban diurnal air temperature variability, but not the average maxima and minima. A range of idealised irrigation scenarios were tested with different rates and timing of watering implemented. Clear evidence was found that irrigation reduces air temperature in urban environments. The diurnal average air temperature was reduced by up to 2.3 °C. The cooling benefit of increasing irrigation was non-linear, with negligible additional cooling predicted above 20 L m^{-2} d^{-1}. The magnitude of cooling was proportional to the pervious (irrigated) fraction, meaning less cooling occurred in areas with greater urban development. Although irrigation increased humidity, it still improved outdoor human thermal comfort during heatwave conditions. IUWM approaches can provide an additional fit-for-purpose water supply to the urban environment, which should be utilised for cooling benefits.

1. Introduction

The warmer climates observed in cities increase the risk to urban dwellers of heat stress and heat related illness. In Australia, where extreme weather and prolonged drought are common, heat exposure in urban areas can be exacerbated. The combination of increasing urban development, excessive urban heating, and lower water availability, alongside the impacts of future climate change could have damaging implications for the health and well-being of urban dwellers. Water management in cities plays an important role in determining urban climates (Coutts et al., 2012; Gober et al., 2010), but minimal work has directly acknowledged these interconnected issues. Integrated urban water management (IUWM), which aims to manage the entire

* Corresponding author at: Arizona State University, School of Geographical Sciences and Urban Planning, Tempe, AZ, USA.
E-mail address: ashley.broadbent@asu.edu (A.M. Broadbent).

http://dx.doi.org/10.1016/j.uclim.2017.05.002
2212-0955/

urban water cycle in an integrated and sustainable way, is growing across Australia. IUWM approaches, including stormwater harvesting and water sensitive urban design (WSUD), provide a means for retaining and using more water in the urban environment. IUWM approaches also have proven positive benefits for a range of hydrological problems including flood mitigation and improved downstream ecology (Walsh et al., 2005). This study examines the potential for irrigation to provide cooling benefits and reduce human exposure to heat stress in the outdoor environment during heatwave conditions.

One of the major drivers of warmer urban temperatures is the lower levels of evapotranspiration (ET) in the urban environment (Oke, 1987). Less ET occurs in urban areas due to widespread impervious surfaces and reduced vegetation coverage. Therefore, increasing vegetation in cities is a commonly cited heat mitigation measure. Urban vegetation is an effective way to reduce urban temperatures (see Bowler et al., 2010, and references therein) . However, vegetation requires ample water to survive and transpire effectively (Clark et al., 1990), which highlights the importance of urban water management for effective heat mitigation. This is especially relevant in Australia where the security of potable water supplies has been threatened by drought and population pressures (Mitchell et al., 2008). The urban water cycle and the availability of water in the urban environment can significantly influence urban temperatures. However, the potential for modulating urban warmth through direct modifications of the urban water cycle, such as by irrigation, has not been considered in great detail.

The most important time to achieve cooling is during extreme heat conditions when urban populations are likely to suffer from heat stress. Thus, irrigation could be used as a targeted heat mitigation measure during a heatwave. IUWM technologies such as bio-filtration systems, rain water tanks, and stormwater harvesting systems could be used for capturing, storing, and treating stormwater and greywater; while irrigation (active or passive) is used to distribute the water to areas where cooling is needed. Grossman-Clarke et al. (2010) examined the effects of irrigation during an extreme heat event at the local-to-mesoscale using the Weather Research and Forecasting (WRF) model. The authors found maximum air temperature (T_a) increased by 2–4 ° C when irrigated agricultural land was converted to suburban development, and urban irrigation caused a 0.5–1.0 ° C cooling of maximum T_a during extreme events. Grossman-Clarke et al. (2010) captured roof-level mesoscale conditions, and not the canopy-layer microscale variability that humans were actually exposed to. A recent study from Daniel et al. (2016), looked at the role of watering practices for future heat-wave risk in Paris. This study utilised atmosphere coupled Town Energy Balance (TEB) model, at 1 km resolution, to look at the aggregated cooling effects of irrigation for hypothetical heatwave conditions. Daniel et al. (2016) found that the best performing night time irrigation scenario could reduce average night time air temperature by 2.6 ° C. Daniel et al. (2016) and Grossman-Clarke et al. (2010) both provide mesoscale assessments of urban cooling from irrigation. However, the possibility irrigation can be used as a heat mitigation measure during extreme conditions, and reduce extreme heat stress at the microscale, has rarely been examined.

Despite the potential for irrigation to provide cooling in urban areas (Coutts et al., 2012; Gober et al., 2010; Grimmond and Oke, 1995; Kalanda et al., 1980; Oke and McCaughey, 1983), it has received a comparatively small amount of attention in the urban heat mitigation modelling literature. Gober et al. (2010) used the Local-Scale Urban Meteorological Parameterization Scheme (LUMPS) (Grimmond and Oke, 2002) and a simple boundary layer model (Oke et al., 1989) to investigate variability in T_a and ET in Phoenix, Arizona. The authors found the rate of night time cooling increased with irrigation because of reduced daytime storage heat. However, this relationship is non-linear, indicating the magnitude of night time cooling levels off when ET rates (and irrigation) are high. This implies adding water is a thermally inefficient strategy for reducing temperatures in well-watered neighbourhoods. This finding was supported by Demuzere et al. (2014) who found a non-linear relationship between ET and irrigation for a bio-filtration system in Melbourne, Australia. As the relationship between ET and cooling is non-linear, the possibility that cooling via irrigation can be optimised should be considered, so that cooling benefits can be maximised and water-use minimised. Two other water-use focused studies utilised a surface energy balance (bulk approach), similar to Gober et al. (2010), including a study from Portland, Oregon (House-Peters and Chang, 2011) and a study conducted in Canberra, Australia (Mitchell et al., 2008). Mitchell et al. (2008) suggest that compared to a landscape with no vegetation at all, a full vegetated WSUD treatment increased summer evaporation by 1.44 to 1.76 mm d^{-1} and could reduce peak afternoon temperatures by up to 4.2 ° C. Overall, these studies reveal important information about the intertwined issues of irrigation and urban climate. However, the spatial and temporal scale and the modelling techniques used in these studies (Gober et al., 2010; House-Peters and Chang, 2011; Mitchell et al., 2008) did not capture the actual human exposure to heat stress in the outdoor environment. Therefore, these studies were not able to directly evaluate the potential for irrigation to reduce human exposure to heat stress during heatwave conditions.

This study examines the potential for irrigation to reduce human exposure (outdoor microscale climate) to extreme heat in a IUWM suburb in South Australia. We utilise the SURFEX (SURFace EXternalisée in French) (Masson et al., 2013) numerical model and high resolution observational data. A model validation was conducted to test model performance against observed data, and the heatwave case study was used to test the effects of different irrigation scenarios on urban microclimate during extreme conditions. Our focus in the present study is the hypothetical cooling effects of irrigation. As such, the approach and experimental design are intended to capture the maximum possible cooling effects of irrigation across the area of interest. The concept of abundantly using water to cool the urban environment during heatwave conditions is in contrast to current outdoor water-use practices in Australia. Due to water scarcity, residents have become highly diligent with their water-use practices, especially during heatwaves and droughts. Therefore, encouraging people to irrigate on a hot day may be counter-intuitive and against normal practice for many residents and local-governments. However, if alternative water is available (i.e. recycled water or stormwater) then water can be justifiably used to cool the urban environment. The rate and timing of irrigation could be modified and tailored to different seasons/environments to achieve highly efficient cooling outcomes. These characteristics of irrigation suggest watering could be an effective approach for cooling urban environments during heatwaves.

2. Data and methods

2.1. Site characterisation

The area of interest for this study is Mawson Lakes (shown in Fig. 1), which is a suburb of Adelaide, South Australia. Adelaide's climate is a hot and dry Mediterranean climate. During summer (December–February), extreme heat events with temperatures exceeding 40 ◦ C are common. The hot and dry conditions that frequently cause heat stress in Adelaide necessitate heat mitigation, but this can be difficult when water supply is limited (February average rainfall = 12.4 mm). Water scarcity has led local governments in Adelaide to utilise IUWM approaches in new developments such as Mawson Lakes. The Mawson Lakes

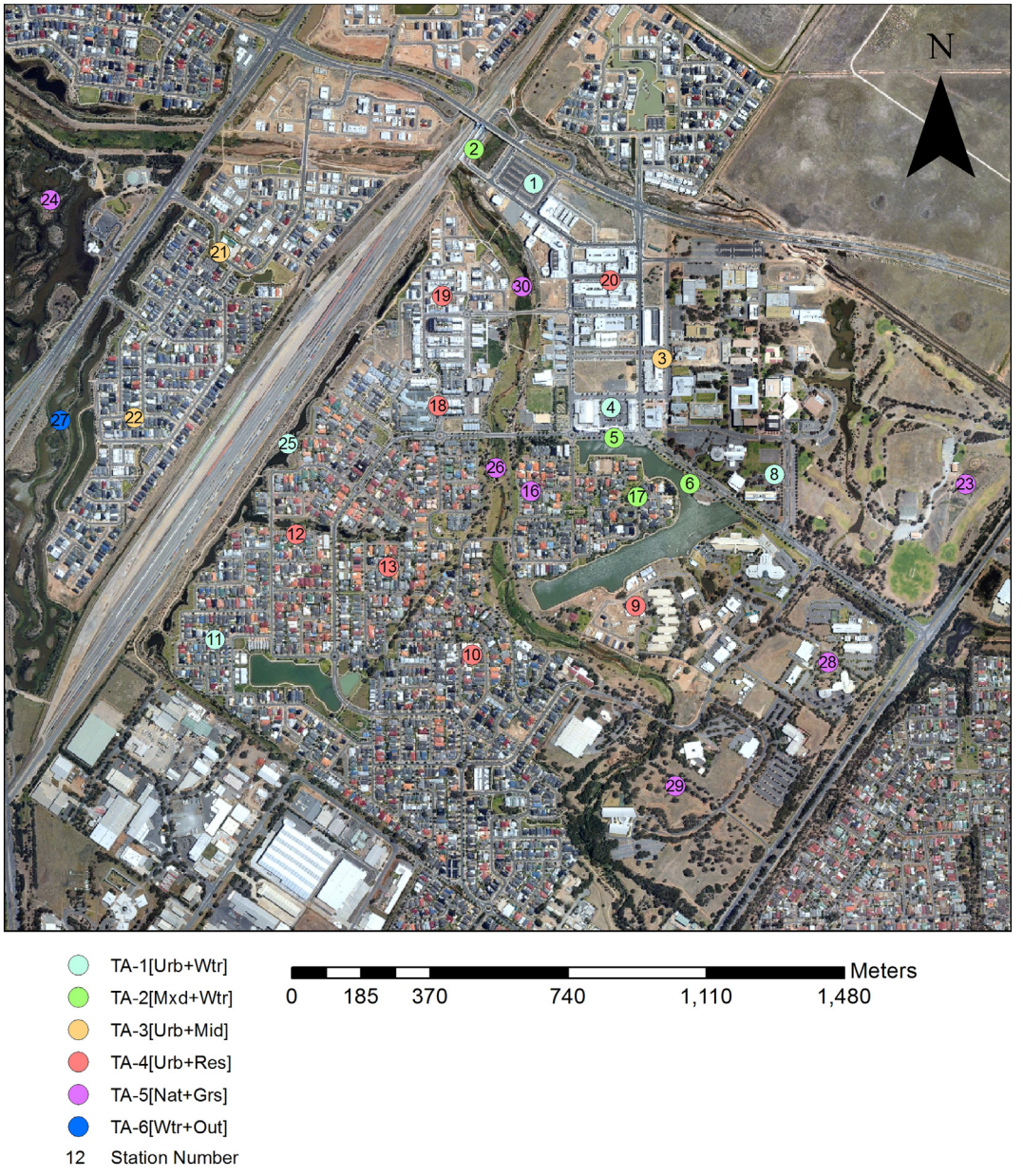

Fig. 1. An overview of Mawson Lake AWS sites with T_a clusters (colour coded) and station numbers indicated. Data from AWS sites (15–17 February 2011) were used for model validation simulations (see Section 3.1). The legend describes clustered AWS sites with statically similar thermally characteristics (Ward hierarchical clustering). These clusters are named accordingly: urban locations near water (TA-$1_{[Urb+Wtr]}$), mixed land cover near water (TA-$2_{[Mxd+Wtr]}$), mid-rise sites (TA-$3_{[Urb+Mid]}$), urban residential (TA-$4_{[Urb+Res]}$), grassy sites (TA-$5_{[Nat+Grs]}$), and an outlier site (TA-$6_{[Wtr+Out]}$).

development is situated 12 km north of Adelaide's central business district. The suburb has medium to low density buildings and consists of open low-rise, open mid-rise, and compact mid-rise local climate zones (Stewart and Oke, 2012). Mawson Lakes is a prototype IUWM development with a sophisticated dual water supply system that includes stormwater harvesting and waste water recycling technologies. A secondary pipe delivers alternative water to the suburb for non-potable uses including irrigation. Much of the public open space in Mawson Lakes, such as parks and recreational areas, is irrigated with non-potable harvested stormwater. Given the IUMW features and alternative water supply available in Mawson Lakes, this suburb could hypothetically utilise irrigation to achieve cooling during heatwave conditions.

2.2. Description of observational data

This research is based on an experimental campaign carried out in Mawson Lakes from 13–17 February 2011. The campaign included the deployment of a dense network of automatic weather stations (AWS) and the acquisition of high resolution remotely sensed data. Synoptic conditions were stable and a land/sea breeze circulation was in place throughout the diurnal cycle. Average wind speed during the observational period was 3.8 ms^{-1}. The T_a was typical for February conditions; the average maximum T_a during the campaign (29.4 ° C) was equal to the long term February average. A small aircraft completed three flights during the Mawson Lakes campaign. The following data were collected: multi-spectral imagery, Light Detection And Ranging (LiDAR) point clouds, and infra-red thermal images. Multi-spectral images were used to generate land cover data (Fig. 2a) and normalised difference vegetation index (NDVI). Land cover categories were derived using a supervised classification technique (maximum likelihood classification in ArcGIS). Sky view factor (SVF) was calculated using the LiDAR data (after Zhu et al., 2013). The remote sensing datasets are used as key inputs for numerical simulations.

Twenty-seven AWS were dispersed across Mawson Lakes (see Fig. 1) to capture microscale variability of T_a in the suburb. The AWS were placed around Mawson Lakes at locations with varying degrees of exposure to IUWM elements. The AWS captured the variability of microclimate in Mawson Lakes and cooling effects of IUWM features. AWS were mounted on metal stakes and street lights at heights of 1.5 –3 m. T_a and relative humidity (RH) were measured using Vaisala HMP155A/HMP45C instruments (accuracy ±0.2° C), and wind speed was observed with RM Young 3-cup anemometers (2% accuracy). The AWS sites were classified into 6 categories using a Ward hierarchical clustering approach (Ward, 1963) (see colour coded clusters in Fig. 1). The daily average, daily minimum, and daily maximum T_a were used as clustering criteria. The T_a derived clusters were named based on the average surface characteristics of each cluster: urban locations near water (TA-$1_{[Urb+Wtr]}$), mixed land cover near water (TA-$2_{[Mxd+Wtr]}$), mid-rise sites (TA-$3_{[Urb+Mid]}$), urban residential (TA-$4_{[Urb+Res]}$), grassy sites (TA-$5_{[Nat+Grs]}$), and an outlier site

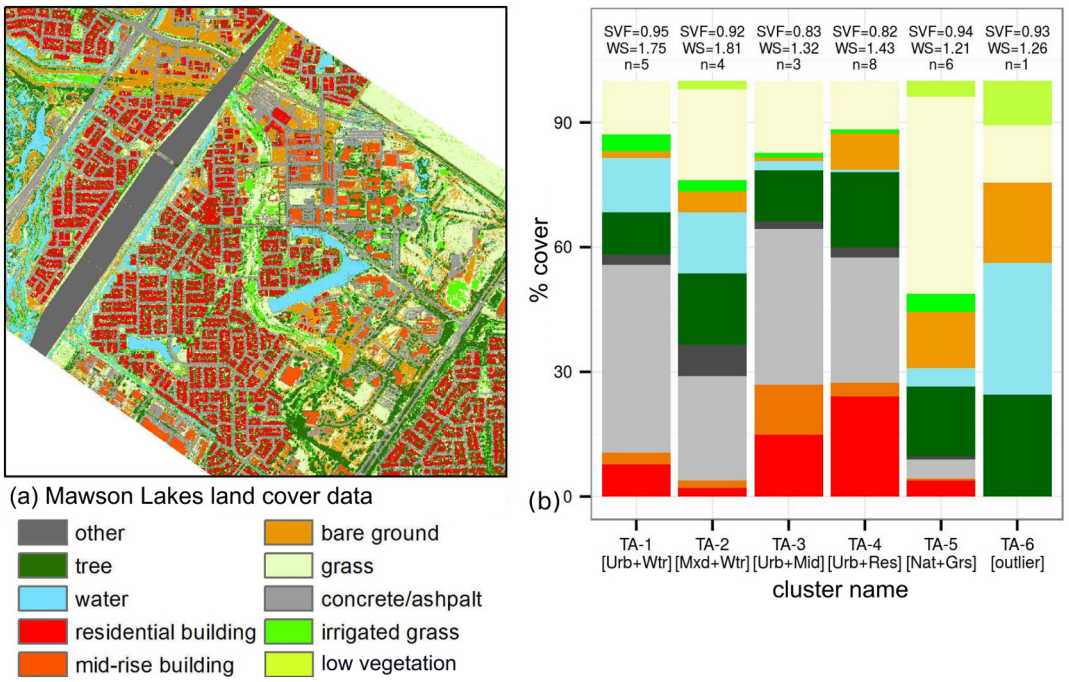

Fig. 2. Overview of (a) land cover data for Mawson Lakes domain and (b) average land cover for AWS clusters. In (b) the cluster average SVF and wind speed (ms^{-1}) are given.

(TA-$6_{[Wtr+Out]}$) (see Fig. 2b). These AWS clusters describe the broad characteristics of intra-suburban T_a variability and are used to assist the validation of SURFEX simulations in the present study.

2.3. SURFEX modelling analysis

2.3.1. SURFEX description

This research used the SURFEX land-surface modelling scheme (Masson et al., 2013) as the primary numerical modelling tool. SURFEX describes the surface fluxes (energy and water) over four major types of surfaces: nature, town, inland water, and ocean. The upper boundary of the model is forced by meteorological data, which can come from an existing modelled or observational dataset (offline) or a coupled atmospheric model (online). This study is concerned with the potential for irrigation to reduce human exposure (microscale climate) to extreme heat. SURFEX was chosen because it is an efficient way to calculate urban canopy layer (UCL) variables and has an adequate representation of the urban water balance (including irrigation representation). For simulating urban surfaces, SURFEX uses the TEB model (Masson, 2000), which is a commonly used urban energy balance model (Masson et al., 2002; Lemonsu et al., 2004; Hamdi and Masson, 2008; Roberts et al., 2006). Traditionally, TEB has been used for neighbourhood scale modelling applications, but the addition of the TEB-Surface Boundary Layer (SBL) scheme (Hamdi and Masson, 2008; Masson and Seity, 2009) and integrated vegetation (TEB-Veg) (Lemonsu et al., 2012b) allows for better simulation of processes inside an urban canyon. In this analysis the TEB-Veg and TEB-SBL schemes were used for simulating meteorological variables inside the UCL. Many surface energy balance models do not take into account urban hydrological processes such as runoff, infiltration, interception, or irrigation (Grimmond et al., 2011, 2010). Representation of irrigation is of critical importance for this research. As such, we used the de Munck (2013) irrigation scheme that has been added to TEB-Veg to simulate outdoor water use. The irrigation regime in TEB-Veg allows for representation of sprinklers, which add extra precipitation to the foliage and soil surfaces inside the canyon, through the following:

$$P_{global} = P + (Irrig \times 24/\Delta t_{Irrig}) = P_{foliage} + P_{soil} \quad (1)$$

where P is the rate of normal precipitation, *Irrig* is the amount of water that would be provided by continuous irrigation, P_{global} is the sum of P and *Irrig*. A fraction of this water is intercepted by the ground and foliage. There is also the possibility in TEB-Veg to represent drip irrigation systems, which only adds the supply of water to the ground. In this study we assume only sprinklers are used.

2.3.2. SURFEX setup

SURFEX was run in offline mode at 25 m resolution (see model domain in Fig. 3) for two separate periods: a model validation period (15 February–17 February 2011) and a heatwave case study period (27 January–7 February 2009). For the model validation period, modified grids were used with each grid cell centred on AWS locations (a 100 m grid was also tested). The 25 m grid shown in Fig. 3 was used during the heatwave case study simulations. We ran the model at 25 m resolution to roughly capture individual urban canyons and the highly localised nature of microclimate characteristics. The orientation of the canyon for all grid points was fixed to observed street orientations (Lemonsu et al., 2012b). The use of 25 m grid meant that a small proportion of grid points in the domain did not correspond to an individual urban canyon (e.g. 100% roof). Accordingly, we checked the model performance against observations at 100 m resolution, and found it performed similarly to the 25 m grid (see Fig. A1 in appendix). There are limitations associated with an offline modelling approach (discussed further in Section 4), but online simulations at this resolution are currently not possible. Advective processes usually reduce the effects of local cooling impacts, thus using an offline approach allowed us to captured the maximum cooling effect of irrigation.

To initialise drought conditions, a 30 day spin up period was used to determine values for surface temperatures and soil moisture. The material characteristics of the urban surfaces in Mawson Lakes were represented using parameters from phase 2 of the PILPS-urban inter-comparison report (see stage 4, Table 2 in Grimmond et al., 2011) . The Grimmond et al. (2011) values were estimated for a suburban site in Melbourne, Australia (Coutts et al., 2007), which is thought to be comparable to the Mawson Lakes domain.

The land cover was defined using the dataset shown in Fig. 2a. In total, 54% of the model domain was classified as pervious (3.74 km^2), 6% open water (0.42 km^2), and 40% was impervious (2.60 km^2). Three patches of vegetation were defined in TEB-Veg using the Mawson Lakes land cover data: permanent broadleaf trees (trees), park areas (grass, irrigated grass, and low vegetation), and bare soil (bare ground). The leaf area index (LAI) for each vegetation patch was defined using values from the literature: broadleaf (eucalyptus) trees a value of 2.4 (Breuer et al., 2003), 1.6 (Grimmond, 1988) for irrigated grass, 0.75 for dry grass, and 3.1 for low vegetation (Breuer et al., 2003). For stomatal resistances the following values were set: broadleaf = 250 m s^{-1} (Breuer et al., 2003), while the park areas and bare soils categories were set at a default value of 40 m s^{-1}. For the soil characteristics the Australian Soil Resource Information System (ASRIS) was used, which provided an average value for Mawson Lakes of 15% clay, 70% sand, and 15% silt. A uniform value for soil type was prescribed across the whole domain, and 3 vertical layers were defined in soil column. Building heights were taken from the LiDAR data; the domain average and

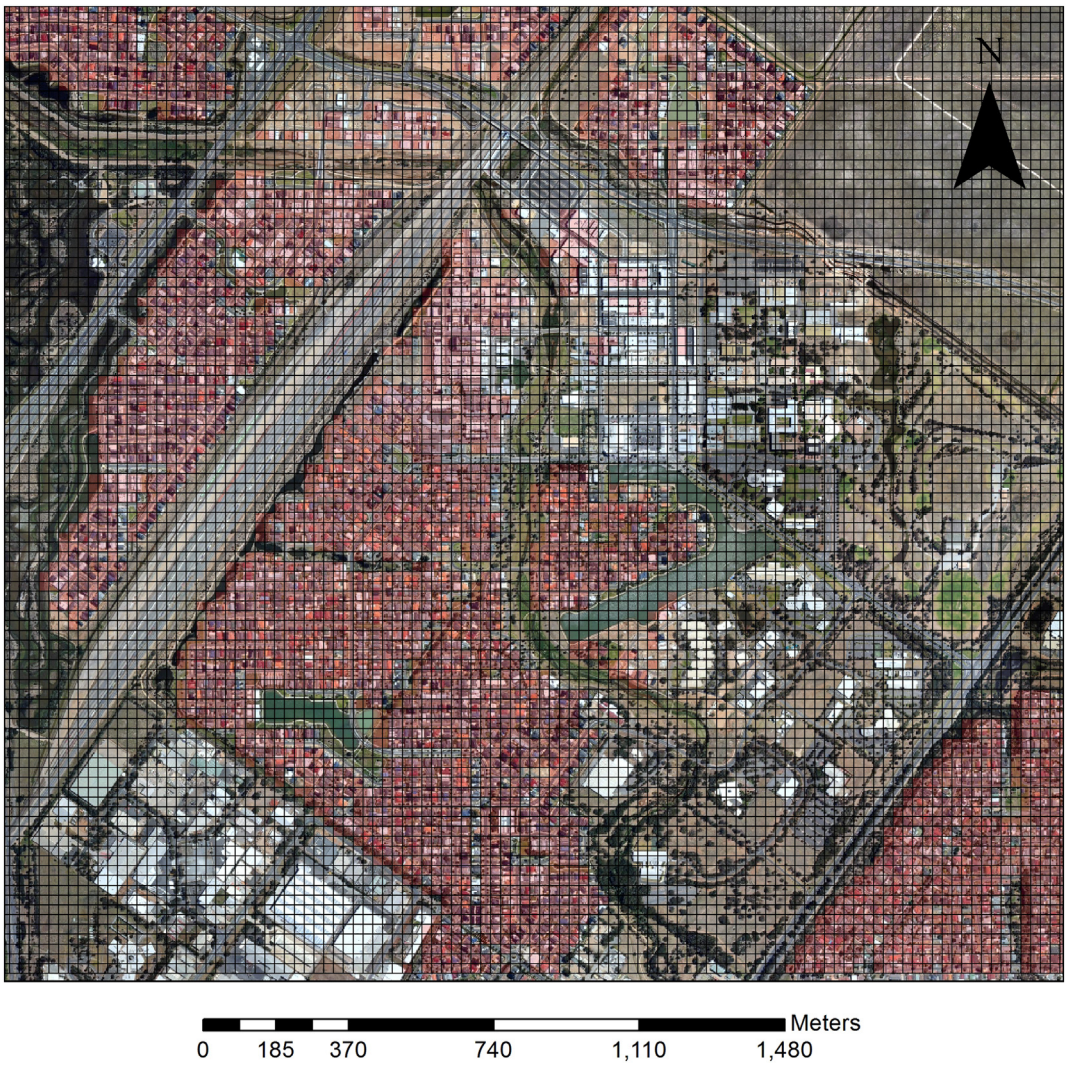

Fig. 3. A map of the Mawson Lakes SURFEX domain (25 m grid) used in this research with residential areas (> 10% residential buildings) shaded red. The grid size is 3100 m (124 cells) × 2600 m (104 cells). This grid setup was used for heatwave case study simulations. For model validation runs, a modified grid was used with 27 cells centred on each AWS (see Fig. 5).

maximum building heights were 4.6 and 11.0 m, respectively. All other land surface parameters not mentioned were left as default as prescribed by the ECOCLIMAP database (Champeaux et al., 2005). Lake surfaces were simulated using the simple lake mode (Masson et al., 2013) and all water bodies were treated as outside the canyon.

2.3.3. Generation of SURFEX forcing data

For each SURFEX simulation a single meteorological dataset was used to force the domain. SURFEX requires atmospheric pressure, incoming longwave radiation, incoming shortwave (direct and diffuse components) radiation, T_a, specific humidity, and wind speed from above roof height. A forcing dataset that was independent from the Mawson Lakes observational data was required to run SURFEX, as the Mawson Lakes data were used for model validation. Surface level meteorological data (excluding radiation variables) were available from the nearby Parafield Airport reference station (Bureau of Meteorology), but data from above roof height were not available. Therefore, we used a simple iterative correction method (Lemonsu et al., 2012a) to generate forcing datasets. SURFEX was run for a single grid point over the Parafield Airport site (hourly model timestep), with a forcing height of 40 m. In the first iteration the model was forced at 40 m using the Parafield Airport near surface meteorological data. The near surface biases were then calculated for the Parafield site, using the difference between the modelled and observed surface values, and the new 40 m forcing data was corrected by subtracting this bias from the previous forcing dataset. Three

successive iterations were performed with SURFEX over the Parafield site. As radiation data were not available from Parafield, data from the Kent Town (Bureau of Meteorology) AWS (approximately 12 km away) were used for the radiation input variables in all simulations.

2.4. Simulation strategy and irrigation scenarios

2.4.1. Heatwave case study

In order to examine the cooling effects of irrigation, SURFEX simulations were conducted for the early 2009 south-eastern heatwave (Fig. 4) (National Climate Centre, 2009). This heatwave affected most of south-eastern Australia and resulted in 13 days of hot weather in Adelaide. During this period, there were 3 days where daily mean T_a exceed 34 ° C (Fig. 4b), which is an Adelaide specific heat health threshold (Loughnan et al., 2013). Using 8 years of data (2004–2012), Loughnan et al. (2013) found that a daily mean $T_a > 34$ °C is correlated with an 8% increase in average mortality in Adelaide (Loughnan et al., 2013). This heatwave case study was used to model the effect of different irrigation scenarios on T_a. The meteorological forcing dataset was taken from the Parafield forcing data (iterative correction method, described in Section 2.3.3) and radiation data came from Bureau of Meteorology Kent Town weather station.

2.4.2. Irrigation scenarios

For the heatwave simulations, a range of irrigation rates were tested with incrementally increasing rates of water-use, to see how changing irrigation affected T_a across the domain. Irrigation was applied to all pervious surfaces (excluding water) in the domain using the de Munck (2013) irrigation module. In this study we only tested irrigation of pervious surfaces, because watering impervious surfaces is against the aims of IUWM and WSUD, which seek to reduce runoff and increase infiltration in urban areas. Nevertheless, urban surfaces can contribute non-negligible amounts of ET in urban areas (Kawai et al., 2010, 2007; Wouters et al., 2015) and future work should consider the cooling effects of irrigating impervious surfaces. Three broad categories of irrigation were simulated, including continuous (24 h), night time (6 h, 11 pm–5 am), and daytime (6 h, 11 am–5 pm) irrigation (Table 1). These scenarios were intended to create an array of irrigation regimes, which would allow for a systematic comparison of different timing and/or rates of water application. The continuous scenarios provided an estimate of the maximum possible cooling that could be achieved for a given rate of irrigation, while the day and night scenarios tested how the timing of irrigation influences microclimate cooling.

Irrigation scenarios represent a hypothetical case of unrestricted water supply, because water was applied to all pervious surfaces in the domain. We acknowledge that most scenarios far exceeded the average outdoor water use for the domain (2.56 ML d^{-1}). Therefore, the scenarios presented, provide an estimate of the maximum cooling from hypothetical irrigation. In reality, we expect that irrigation would be used selectively across the domain, and therefore much less total water would be consumed. However, by using an offline approach and applying water to all pervious surfaces we capture the maximum hypothetical cooling effects of irrigation across different environments.

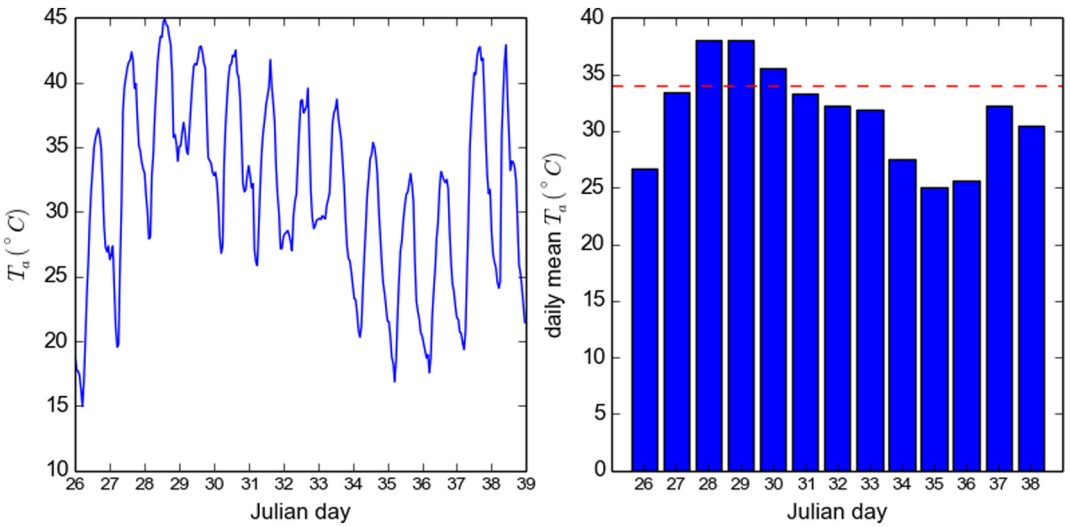

Fig. 4. An overview of the heatwave case study period 26 January–8 February 2009: (a) a time series of hourly average T_a and (b) the daily mean T_a with a heat health threshold of 34 °C (Loughnan et al., 2013) indicated. There were three days during the heatwave that exceeded the heat health threshold: 28, 29, and 30 January.

Table 1
A description of 24h (continuous) irrigation scenarios used in this study.

Scenario	Hourly irrigation ($L\,m^{-2}\,h^{-1}$)	Daily irrigation ($L\,m^{-2}\,d^{-1}$)	Water-use (domain)[a] ($ML\,d^{-1}$)	Water-use (residential) ($ML\,d^{-1}$)
24Irr5L	0.21	5	17.6	3.8
24Irr10L	0.42	10	35.1	7.6
24Irr15L	0.63	15	52.7	11.5
24Irr20L	0.83	20	70.2	15.3
24Irr30L	1.25	30	105.3	22.9
Day_6Irr1.25L | Night_6Irr1.25L	0.21	1.25	4.4	1.0
Day_6Irr2.5L | Night_6Irr2.5L	0.42	2.50	8.8	1.9
Day_6Irr3.75L | Night_6Irr3.75L	0.63	3.75	13.2	2.9
Day_6Irr5L| Night_6Irr5L	0.83	5.00	17.6	3.8
Day_6Irr7.5L | Night_6Irr7.5L	1.25	7.50	26.3	5.7
Day_6Irr10L | Night_6Irr10L	1.67	10.0	35.1	7.6
Day_6Irr12.5L | Night_6Irr12.5L	2.08	12.5	43.9	9.6
Day_6Irr25L | Night_6Irr25L	4.17	25.0	87.8	19.2

Day scenarios=11am–5pm.
Night scenarios=11pm–5am.
ML=mega-litres.
[a] Note that these simulations are hypothetical and in reality irrigation would be conducted selectively. We irrigated the whole domain to assess the effect of irrigation across a range of suburban environments.

3. Results and discussion

3.1. Model validation

To validate the model, SURFEX output (2 m canyon T_a) was compared with observed T_a from Mawson Lakes (see Fig. 1 for AWS locations) for the period 15 February–17 February 2011. To determine model performance of intra-suburban T_a variability, we assess model accuracy against 6 AWS clusters (shown in Fig. 5). The AWS clusters represent groups of sites with thermally similar characteristics. Water affected sites (TA-$1_{[Urb+Wtr]}$ and TA-$2_{[Mxd+Wtr]}$) were observed to be 0.25–0.5 ° C cooler than the suburb average during the day. While urban sites (TA-$3_{[Urb+Mid]}$ and TA-$4_{[Urb+Res]}$) were 0.5–1 ° C warmer than the domain throughout the entire diurnal cycle. The TA-$5_{[Nat+Grs]}$ cluster was characterised by a typical rural thermal regime, including daytime-heating and rapid night-time-cooling. TA-$6_{[Wtr+Out]}$ was a single location that had anomalously cool conditions throughout the diurnal cycle. The average observed minimum and maximum T_a for each cluster are given in Table 2.

Overall, the intra-suburban variability between clusters was not completely captured by the model. The diurnal average T_a of each cluster was reasonably well captured, but the model showed less skill at capturing the daily average minima and maxima. The average maximum T_a was over-predicted for all 6 clusters, but the relative differences in daily maxima were broadly captured. Further, the intra-suburban range of modelled maximum T_a (2.1 ° C) was in-line with observations (2.4 ° C); suggesting the model is broadly capturing the dynamics of daily maximum T_a.

Daily minimum T_a was the worst performing variable tested, with little difference (0.2 ° C) in minimum T_a between clusters, and consistent under-predictions of minimum T_a. The reason for this lack variability in daily minima is unclear, but may be related to inaccuracies or unrepresentative values in the parameters used. We assumed homogeneous urban and vegetation parameters across all locations. Key differences in thermal properties of urban materials and soil moisture heterogeneity may have contributed to model inaccuracies, especially at this fine scale. However, model parameters cannot explain why the minimum T_a for TA-$5_{[Nat+Grs]}$ was not substantially cooler than TA-$3_{[Urb+Mid]}$, given the large differences in pervious fraction between those groups (Fig. 2b). We suspect this may reflect a flaw in the methodology we used to derive the forcing dataset, and/or that TEB-Veg (which was used for the whole domain) is not well suited to simulating a grid cell with a building fraction near zero (i.e. TA-$5_{[Nat+Grs]}$ sites). A non-integrated vegetation model, such as integrated-soil-biosphere-atmosphere (ISBA) model, may be better suited for capturing the thermal characteristics of open sites.

As has been noted, the offline approach neglects advective processes, and T_a is calculated using only the directly adjacent surface characteristics (i.e. 25 m grid) as surface inputs. We tested if model performance was improved by running the model at a coarser (100 m) resolution. We found that model performance at 100 m was similar to the 25 m grid, with the exception of TA-$6_{[Wtr+Out]}$, TA-$1_{[Urb+Wtr]}$, and TA-$2_{[Mxd+Wtr]}$, which were more accurately modelled at 25 m resolution. Overall, we found that the 25 m grid provided more accurate results, especially for sites that were directly adjacent water bodies.

Overall, we conclude that SURFEX cannot fully capture the intra-suburban T_a variability in Mawson Lakes. We ran that model and 25 m and 100 m resolution and both simulations failed to fully capture the variability, although the 25 m run performed better. The model was able to broadly capture the variability in average diurnal T_a across the domain. However, the daily minima and maxima were less accurately captured. The model deficiencies could be due to the forcing dataset used; heterogeneity of model parameters not captured; and limitations associated with the use of TEB-Veg in open areas. Future work should explore these factors, as capturing intra-urban variability is important for impact studies. We now use the SURFEX model to investigate

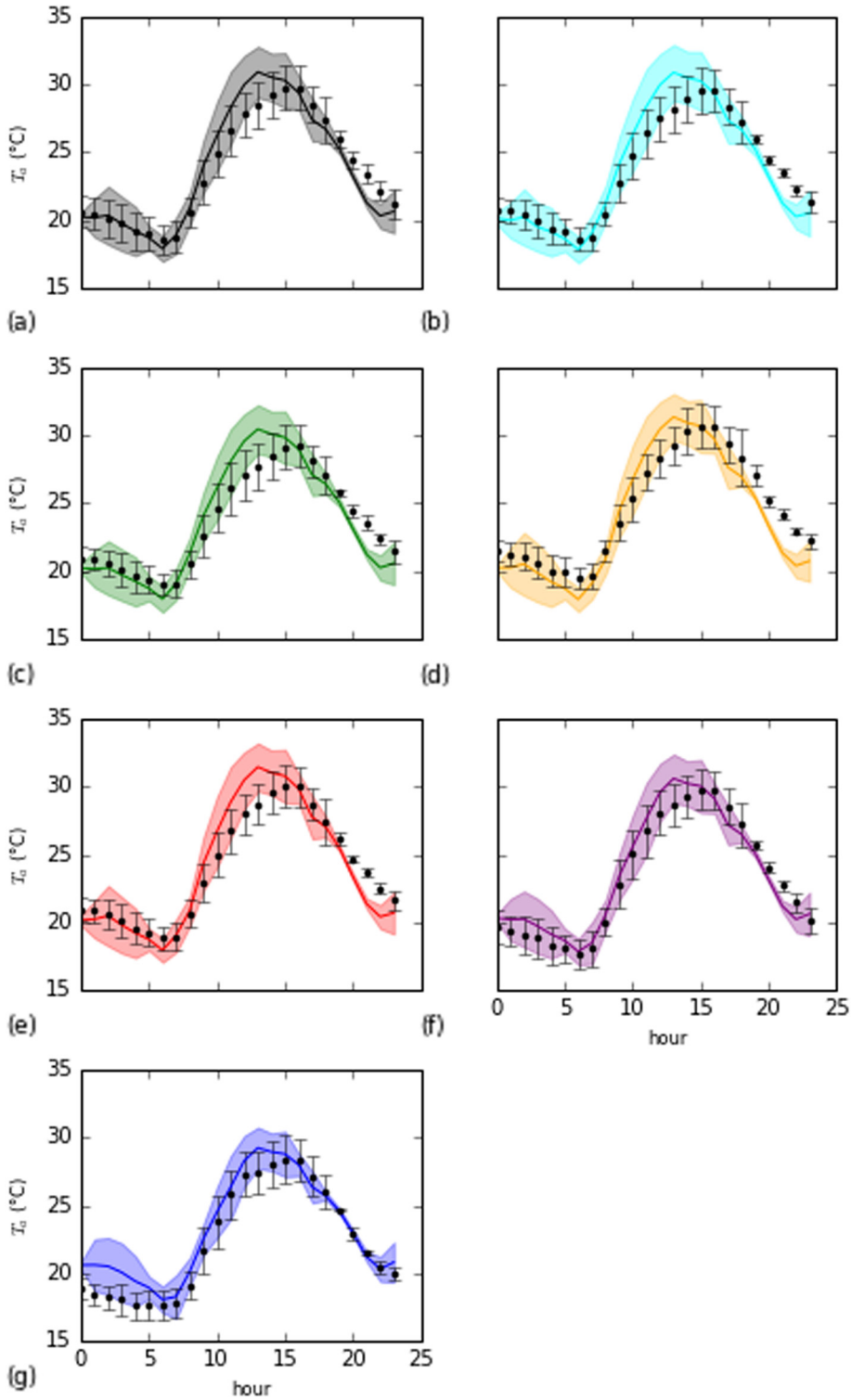

Fig. 5. The diurnal average modelled (lines) vs. observed (bars) 2 m T_a during observational period (15–17 February), for a 25 m grid, grouped by T_a cluster: (a) all AWS sites, (b) TA-$1_{[Urb+Wtr]}$ (c) TA-$2_{[Mxd+Wtr]}$, (d) TA-$3_{[Urb+Mid]}$, (e) TA-$4_{[Urb+Res]}$, (f) TA-$5_{[Nat+Grs]}$, and (g) TA-$6_{[Wtr+Out]}$ (see Fig. 3 for AWS clusters). Standard deviations are shown for both modelled and observed values.

Table 2
The statistical validation of SURFEX for AWS clusters in Mawson Lakes.

Cluster	n	r	$RMSE$	$T_{a[o]}$ (diurnal)	$T_{a[m]}$ (diurnal)	$T_{a[o]}$ (max)	$T_{a[m]}$ (max)	$T_{a[o]}$ (min)	$T_{a[m]}$ (min)
TA-$1_{[Urb+Wtr]}$	330	0.94	1.8	23.7 ± 4.0	23.8 ± 4.8	29.7	31.3	18.5	17.6
TA-$2_{[Mxd+Wtr]}$	264	0.94	1.7	23.6 ± 3.8	23.7 ± 4.6	29.4	30.8	18.9	17.8
TA-$3_{[Urb+Mid]}$	198	0.94	1.7	24.5 ± 4.1	24.1 ± 4.9	30.9	31.8	19.4	17.8
TA-$4_{[Urb+Res]}$	528	0.95	1.6	24.0 ± 4.1	24.1 ± 4.9	30.2	31.8	18.7	17.8
TA-$5_{[Nat+Grs]}$	396	0.94	1.6	23.3 ± 4.6	23.6 ± 4.6	29.9	31.0	17.4	17.6
TA-$6_{[Wtr+Out]}$	66	0.95	1.6	22.4 ± 4.3	23.2 ± 4.0	28.5	29.7	17.5	17.7
All sites	1782	0.94	1.7	23.7 ± 4.2	23.9 ± 4.8	29.9	31.3	18.4	17.7

$T_{a[o]}$ = mean observed air temperature.
$T_{a[m]}$ = mean modelled air temperature.
r = correlation coefficient.
$RMSE$ = root mean square error.

the effect of irrigation on T_a across the whole domain during a heatwave case study period. Given the performance of the model outlined above, results from the heatwave simulations are carefully interpreted. Importantly, we assume that modelled diurnal average T_a is more reliable than the daily minimum and maximum T_a.

3.2. Heatwave simulations

3.2.1. Base case

The base case heatwave simulation shows the T_a variability in Mawson Lakes during heatwave conditions without any irrigation. The average spatial variability of 3 pm and 3 am T_a throughout the entire heatwave is shown in Fig. 6. The modelled night time (3 am average) variability during the heatwave was much smaller than the day (3 pm average), with approximately 1.5 ° C of variability across the domain (Fig. 6b). The natural areas were 0.5–0.75 ° C cooler than urbanised areas at night. Given the findings from the model validation, this is likely represents an under-prediction of nocturnal T_a variability. By contrast, the average 3 pm T_a varied across the domain by as much as 9 ° C; areas near water bodies were below 30 ° C and urbanised areas reached 37 ° C. Water bodies aside, the majority of locations in the domain, including urbanised areas (e.g. x = 70, y = 40 in Fig. 6a) and open grassy areas (e.g. x = 110, y = 60 in Fig. 6a), were very hot at 3 pm. Although vegetated areas were slightly cooler (0.5 ° C) than urbanised sites, most of the domain reached an average 3 pm $T_a > 35$°C during the heatwave. In the base case simulation the initial conditions (i.e. drought) and the lack of irrigation meant all vegetated areas were dry and provided little daytime cooling benefit. This illustrates the need to irrigate vegetation, in order to maximise cooling benefits from greenspace during hot conditions.

3.2.2. Cooling benefits of irrigation and temporal variability

Continuous irrigation. The results from the continuous (24 h) irrigation scenarios show the maximum hypothetical cooling that could be achieved by integrating water into the urban environment during a heatwave. Across the entire heatwave period,

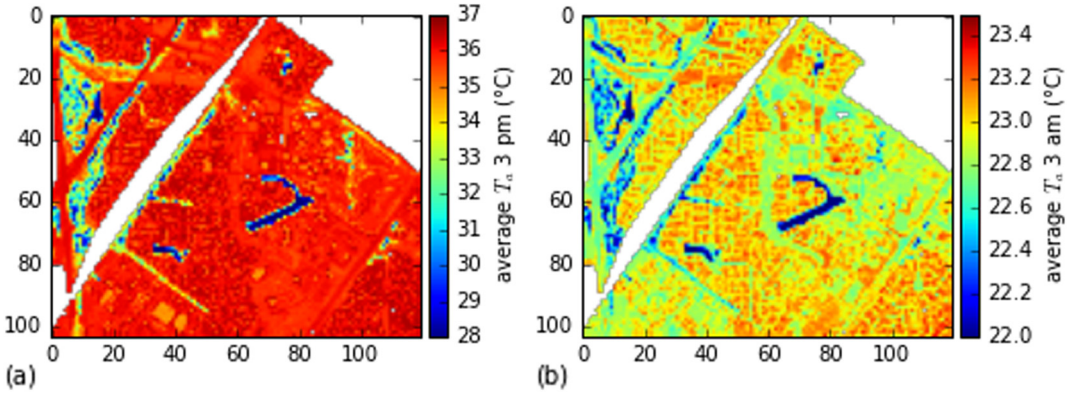

Fig. 6. The spatial representation of the heatwave average (a) 3 pm and (b) 3 am T_a (2 m) across the Mawson Lakes domain for the base case (no irrigation) simulation. The x and y axes are labelled by cell number.

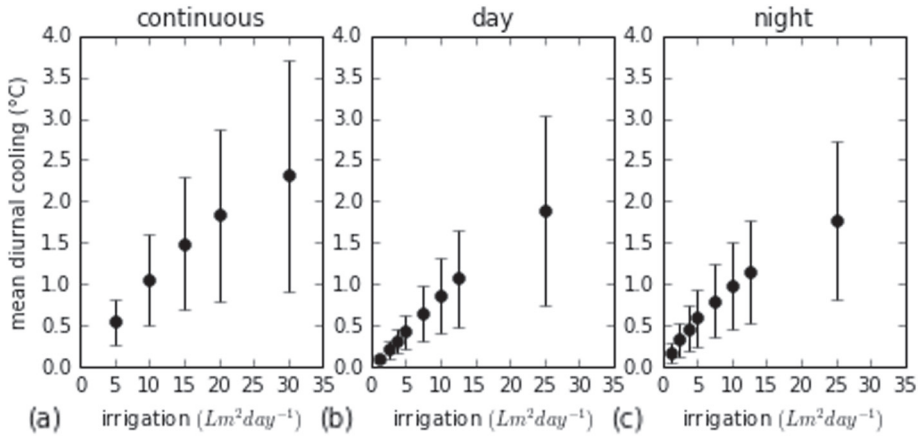

Fig. 7. Heatwave average diurnal cooling (with standard deviations) for (a) continuous, (b) day, and (c) night irrigation.

continuous irrigation resulted in average diurnal cooling of up to 2.31 ° C (Fig. 7a). The irrigation scenarios show, as observed by others (Demuzere et al., 2014; Gober et al., 2010), there is a non-linear relationship between irrigation and diurnal T_a cooling. T_a cooling begins to plateau when the surface soil becomes saturated and maximum ET is occurring based on atmospheric demand. This implies that irrigation volume and timing can be optimised to achieve maximum efficiency of cooling.

The average diurnal cooling varied from day-to-day during the heatwave (Fig. 8a). More diurnal average cooling occurred on hotter days (e.g. 27–30 and 37), primarily due to higher atmospheric demand for ET. Julian day 37 received largest amount of cooling because it was a very hot day that was proceeded by three days of less extreme conditions (Fig. 8), allowing additional water to accumulate in the soil column. This demonstrates the potential cumulative benefits of irrigation, and implies that irrigation before a heatwave (we assumed no irrigation pre-heatwave) may provide additional cooling benefits. Spatial plots of cooling on Julian day 37 (Fig. 9) show significant spatial and temporal variability of cooling, due to pervious fraction and vegetation type (discussed further below). For continuous irrigation, more cooling occurred during day hours than at night (Fig. 9).

Cooling during the day was primarily driven by a large increase in the latent heat flux. The domain average 3 pm Bowen ratio decreased from 5.7 (without irrigation) to −0.05 with heavy irrigation (24Irr30L). For the 24Irr30L scenario, the average 3 pm latent heat flux was equal to net radiation and the sensible heat flux became slightly negative (−40 W m^{-2}), indicating the surface was cooler than the atmosphere during the day (oasis effect). In reality, if irrigation was conducted across the entire domain, the oasis effect would not have been this strong because of land surface-atmosphere feedbacks. Previous research has found different model sensitivity to surface energy balance changes when comparing coupled and offline TEB simulations (Krayenhoff and Voogt, 2010). In our study, the use of a static atmospheric forcing (no feedback between the atmosphere and land surface)

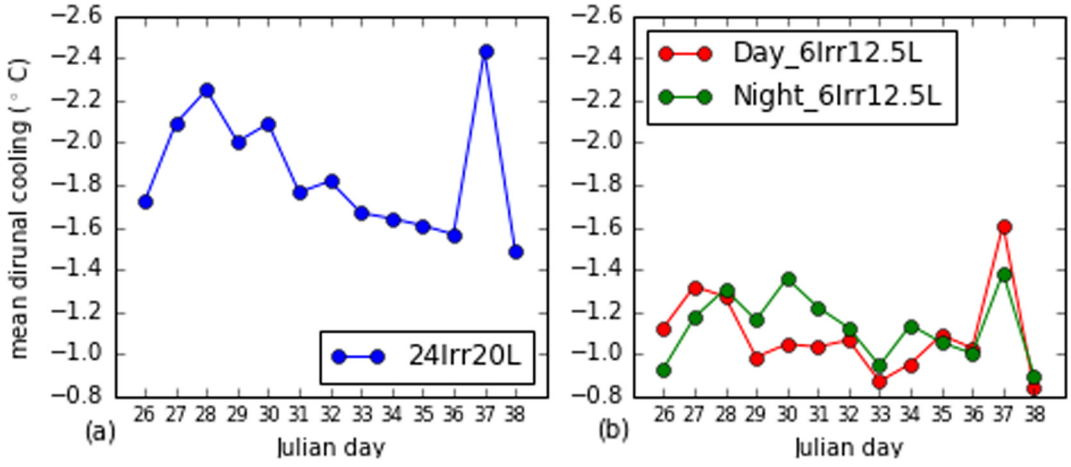

Fig. 8. Diurnal average for each day during the heatwave for (a) 24Irr20L and (b) Day/Night_6Irr12.5L scenarios.

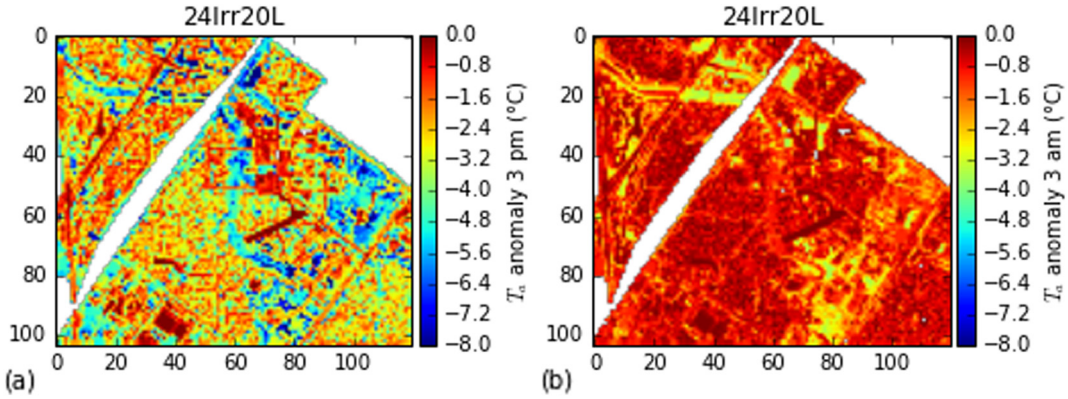

Fig. 9. Spatial representation of cooling from 24Irr20L at (a) 3pm and (b) 3am on Julian day 37. The x and y axes are labelled by cell number.

likely caused an over-prediction of surface-level ET, because reference level atmospheric humidity (and temperature) did not increase (decrease) in response to irrigation. Thus, for the higher irrigation scenarios (where strong feedback occurs), these results represent the effects of irrigating a small area that is surrounded by dry unirrigated surfaces.

The model suggests that night time cooling was primarily driven by an increase in the latent heat flux, which was positive for all irrigation scenarios (up to 80 W m^{-2} for 24Irr30L). The positive latent heat flux indicates a nocturnal evaporative cooling effect with irrigation. Previous research suggests ET can occur at night (Konarska et al., 2016). However, future work should assess if this magnitude is plausible for an isolated patch of heavily irrigated vegetation during extremely hot and dry conditions.

Day and night irrigation. Another two sets of irrigation scenarios were tested to compare the cooling effects of night and day irrigation. The volume of water used in these scenarios was 25% the volume of the continuous irrigation scenarios. Daytime irrigation provided more cooling during the day, and night time irrigation provided greater cooling at night (Fig. 10). However, the average diurnal cooling provided by night and day irrigation was more complicated. Firstly, average diurnal cooling from day irrigation increased linearly (Fig. 7b), while night time irrigation did not (Fig. 7c). Additionally, night time irrigation provided marginally more diurnal cooling than daytime irrigation for all scenarios using less than 25 L m^{-2} d^{-1}. This occurred because the cooling benefits of night time irrigation extend for a longer period post-irrigation. However, daytime irrigation was more effective at cooling diurnal average T_a for the maximum irrigation rate tested (25 L m^{-2} d^{-1}). This greater cooling with Day_6Irr25L occurred because during the day water was quickly evapotranspired away from the surface, and a large volume of daytime irrigation was required to see a post-irrigation night time cooling benefit. Overall, the night and day scenarios highlight the complexity of irrigation timing dynamics; more analysis is needed in this area, but these results indicate there is potential to optimise the timing and volume of irrigation for thermal benefits.

3.2.3. Spatial variability of cooling

Within the domain there was spatial variability of cooling from irrigation, which was primarily driven by the amount of pervious area available to apply water. For the 24Irr20L scenario, average diurnal cooling increased at a near linear rate as pervious fraction increased (Fig. 11). For the 24Irr20L scenario, a 10% increase in irrigated pervious fraction equates to a cooling of 0.25 ° C (daily average temperature). In the spatial data, it is clear that areas with more pervious surfaces (and therefore more irrigation) were cooler during the heatwave (Figs. 9 and 10). On Julian day 37, for the 24Irr20L scenario, the heatwave average 3 pm T_a of highly pervious areas, cooled by up to 9 ° C, while residential areas only cooled 1–3 ° C (see Fig. 9a).

Fig. 9 also indicates that the spatial variability of vegetation type contributed to T_a variability. Most notably, areas with a high proportion of bare ground produced large cooling benefits (e.g. x = 40, y = 20 in Fig. 9). This occurred because, prior to irrigation, bare ground surfaces were extremely dry, and thus received a greater evaporative cooling effect. Bare ground also had minimal infiltration and uptake of water from plants, allowing for very rapid evaporation of surface water to occur. For 24 h irrigation, the continuous supply of water meant a large cooling effect occurred over bare ground. However, when non-continuous (6 h) irrigation was conducted, bare ground dried out faster (Fig. 10b) and provided less sustained cooling. By contrast, well vegetated surfaces (with higher LAI) provided more sustained cooling effects (e.g. x = 100, y = 55 in Fig. 10c), as some water is stored and evapotranspired later, rather than being immediately evaporated. This suggests greener and healthier vegetation will provide more prolonged cooling from when irrigation is not continuously applied. There are important differences in the magnitude and timing of cooling provided by irrigation over different vegetation and soil types. This area requires future research in order to further optimise the cooling benefits of irrigation during extreme heat.

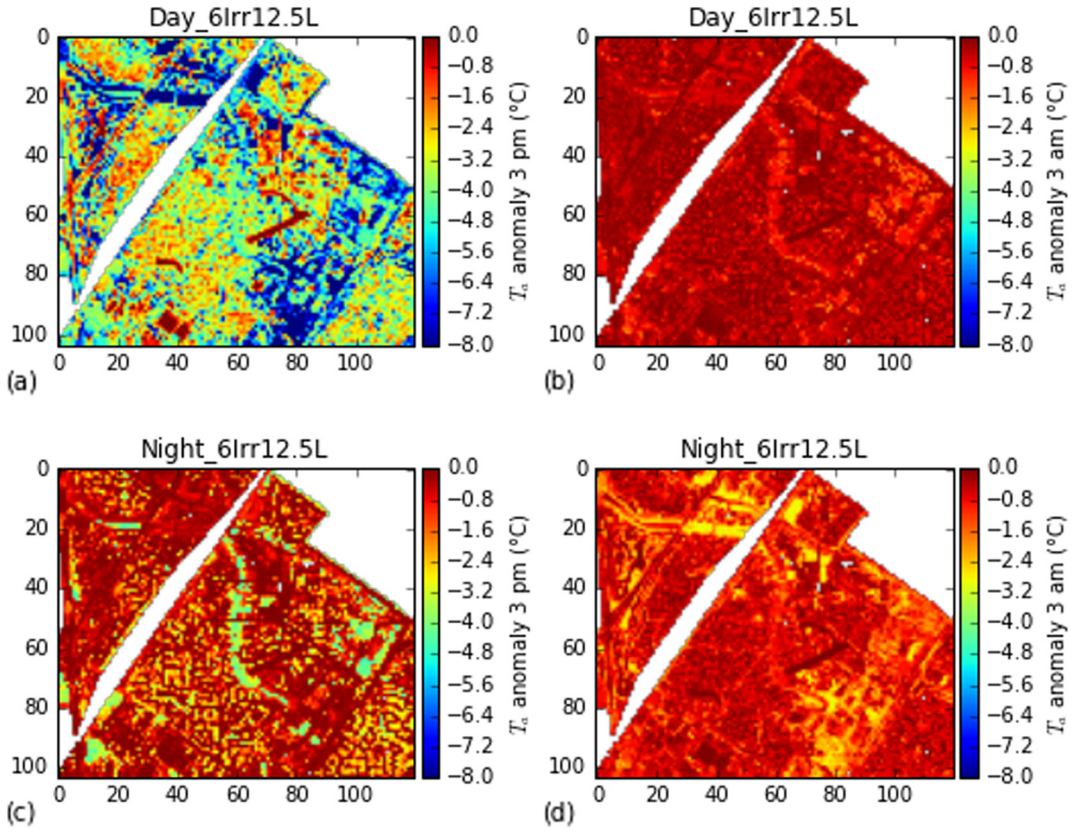

Fig. 10. Spatial representation of cooling from Day/Night_6Irr12.5L scenario at (a/c) 3pm and (b/d) 3am on Julian day 37. The x and y axes are labelled by cell number.

3.2.4. Irrigation efficiency

To do determine irrigation cooling efficiency, we calculated the spatial field of cumulative cooling for the heatwave duration, expressed on one average day (Daniel et al., 2016):

$$\Delta Tm^{SCE}(d,i) = \frac{\sum_{h=1}^{h=24*d} (Tm^{SCE}(h,i) - Tm^{REF}(h,i))}{d} \tag{2}$$

where d is days, h is hours, i is the spatial index for each grid cell, Tm^{SCE} and Tm^{REF} are the modelled scenario and reference 2 m T_a. To look at irrigation cooling efficiency of difference surfaces, $\Delta Tm^{SCE}(d,i)$ was spatially averaged and normalized according to different SURFEX land cover types after Daniel et al. (2016):

$$\Delta Tm^{SCE}_{surf}(d) = \frac{\sum_{h=1} (\Delta Tm^{SCE}(d,i) f_{surf}(i))}{\sum_{h=1} f_{surf}(i)} \tag{3}$$

where $f_{surf}(i)$ is the fraction of the surface type in question. We calculate $\Delta Tm^{SCE}_{surf}(d)$ for the whole domain ($\Delta Tm^{SCE}_{all}(d)$), building fraction ($\Delta Tm^{SCE}_{bld}(d)$), park fraction ($\Delta Tm^{SCE}_{park}(d)$), tree fraction ($\Delta Tm^{SCE}_{tree}(d)$), and bare ground fraction ($\Delta Tm^{SCE}_{bare}(d)$). The cooling efficiency of irrigation is then computed as (Daniel et al., 2016):

$$Ef_{surf} = \frac{\Delta Tm^{SCE}_{surf}(d)}{V_{wtr(SCE)}} \tag{4}$$

where $V_{wtr(SCE)}$ is the spatially averaged water-use volume for the irrigation scenario. The Ef_{surf} results for all irrigation scenarios are given in Table 3.

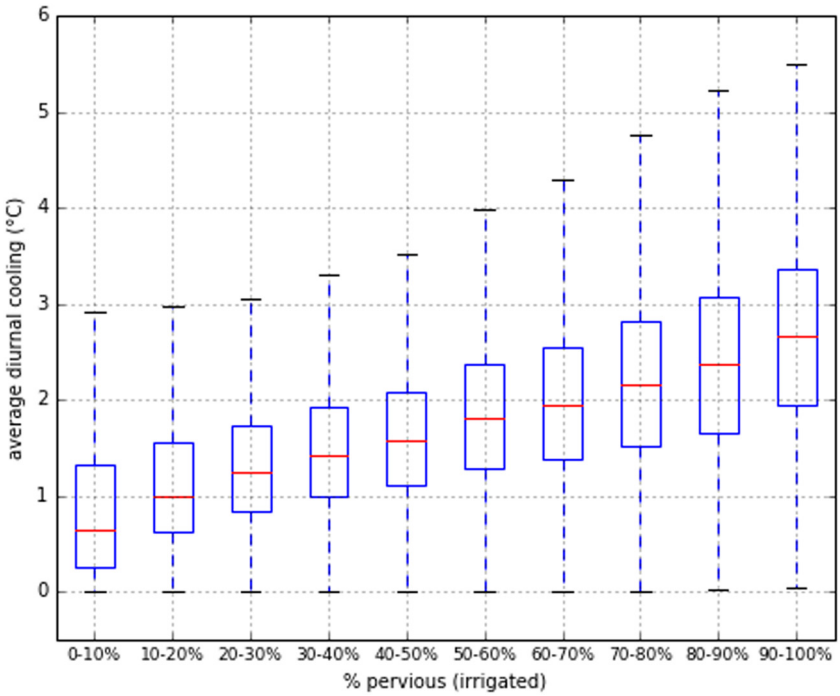

Fig. 11. The daily cooling (24Irr20L scenario) for each grid cell during the heatwave period grouped by pervious (irrigated) fraction. Average cooling increases at a near linear rate, but does diminish slightly above 90% perviousness. The boxes in this figure represented the inter-quartile range and the whiskers represent 1.5 × inter-quartile range.

Firstly, focussing on the Ef_{all}, these results confirm observations discussed above; that irrigation efficiency decreases as the total volume of water-use increases. As noted, the exception to this is daytime irrigation, which does not decrease in efficiency as water use increases. These results also confirm that night time irrigation is more efficient than daytime irrigation at water-use below 25 L m $^{-2}$.

Table 3
Average Ef_{surf} (see Eqs. 2–4) from irrigation (°C L^{-1}) normalized by surface type.

Scenario	Ef_{all}	Ef_{park}	Ef_{tree}	Ef_{bare}	Ef_{bld}
d25HW5	−0.0094	−0.0106	−0.0105	−0.0121	−0.0076
d25HW10	−0.0090	−0.0103	−0.0101	−0.0122	−0.0070
d25HW15	−0.0085	−0.0096	−0.0096	−0.0119	−0.0065
d25HW20	−0.0078	−0.0087	−0.0089	−0.0113	−0.0058
d25HW30	−0.0066	−0.0072	−0.0075	−0.0098	−0.0047
Day_6Irr1.25L	−0.0067	−0.0078	−0.0074	−0.0082	−0.0054
Day_6Irr2.5L	−0.0071	−0.0081	−0.0078	−0.0085	−0.0059
Day_6Irr3.75L	−0.0072	−0.0083	−0.0080	−0.0086	−0.0061
Day_6Irr5L	−0.0073	−0.0084	−0.0081	−0.0088	−0.0061
Day_6Irr7.5L	−0.0074	−0.0085	−0.0082	−0.0091	−0.0061
Day_6Irr10L	−0.0074	−0.0085	−0.0083	−0.0094	−0.0059
Day_6Irr12.5L	−0.0073	−0.0085	−0.0082	−0.0097	−0.0056
Day_6Irr25L	−0.0064	−0.0073	−0.0074	−0.0094	−0.0047
Night_6Irr1.25L	−0.0117	−0.0131	−0.0132	−0.0160	−0.0089
Night_6Irr2.5L	−0.0112	−0.0127	−0.0127	−0.0162	−0.0082
Night_6Irr3.75L	−0.0106	−0.0120	−0.0120	−0.0151	−0.0079
Night_6Irr5L	−0.0100	−0.0113	−0.0113	−0.0142	−0.0075
Night_6Irr7.5L	−0.0091	−0.0102	−0.0102	−0.0127	−0.0069
Night_6Irr10L	−0.0084	−0.0095	−0.0095	−0.0117	−0.0064
Night_6Irr12.5L	−0.0079	−0.0089	−0.0089	−0.0109	−0.0059
Night_6Irr25L	−0.0060	−0.0068	−0.0068	−0.0084	−0.0045

The irrigation efficiency for different surface types also provides some interesting insights. For all irrigation scenarios bare ground provided the highest irrigation efficiency (Table 3) compared to trees and park surfaces. Thus, the model suggests that the greatest amount of cumulative cooling occurs when very dry surfaces are irrigated. This effect over bare ground is particularly apparent in the day irrigation scenarios; Ef_{bare} did not significantly decrease as water-use increased. This finding implies that although bare ground does not provide as prolonged cooling effects (Fig. 10c), the total cumulative cooling is greater than vegetated surfaces. Further, this suggests that irrigation of impervious surfaces (e.g. asphalt), which are similar to bare ground, could be an efficient means of achieving cooling in built-up areas.

Lastly, Ef_{bld} was lower than all other surfaces tested. This is not surprising as only pervious surfaces were irrigated in our scenarios, and therefore, the magnitude of cooling in built-up areas is constrained by the available pervious fraction. Thus, the approach to calculate irrigation efficiency used above, actually partially obscures the true efficiency of irrigation in built-up areas. Given that only pervious surfaces were irrigated, to get a better measure of irrigation efficiency in built-up areas, we divide the domain into two zones: residential (see Fig. 3) and non-residential (defined as all non-residential grid points). We then calculated the irrigation efficiency of each zone using:

$$Ef_{zone} = \frac{\sum_{i} \Delta Tm^{SCE}_{zone}(d,i)}{\sum_{i} V_{zone}(i)} \tag{5}$$

where $V_{zone}(i)$ is the total daily water-use for grid cell i in the given zone. Thus, Eq. (5) is the sum of daily cumulative cooling across the zone divided by the total daily water-use in the zone. Irrigation in the residential zone was 20–40% more efficient at providing cooling (Table 4) per L of water applied. The increased efficiency of cooling in urban areas was likely driven by higher urban temperatures in urban areas. These results imply that, even when only pervious surfaces are irrigated, residential areas can receive more cooling per L of irrigation than open areas, but that total magnitude of cooling is constrained in residential areas by that available pervious fraction.

3.3. Implications for population

3.3.1. Heat health thresholds

The spatial variability of microscale T_a shown in the irrigation scenarios presented (Fig. 9), indicate there are areas within the domain (such as more urbanised sites) where people experience hotter temperatures during heatwaves. To understand this spatial variability further, we calculated the percentage of the domain (whole domain and residential areas [Fig. 3]) that exceeded a

Table 4
Zone average irrigation cooling efficiency (Ef_{zone}). Ef_{zone} is the zone sum of $Tm^{SCE}(d, i)$ divided by the total water use in the zone.

Scenario	(Ef_{res}) (°C L^{-1})	(Ef_{nores}) (°C L^{-1})	$\Delta\%Ef_{res} - Ef_{nores}$ (%)
d25HW5	−0.0101	−0.0072	34
d25HW10	−0.0093	−0.0070	28
d25HW15	−0.0086	−0.0067	26
d25HW20	−0.0077	−0.0062	21
d25HW30	−0.0063	−0.0053	17
Day_6Irr1.25L	−0.0073	−0.0051	36
Day_6Irr2.5L	−0.0080	−0.0053	41
Day_6Irr3.75L	−0.0082	−0.0054	42
Day_6Irr5L	−0.0083	−0.0055	41
Day_6Irr7.5L	−0.0082	−0.0056	38
Day_6Irr10L	−0.0079	−0.0056	33
Day_6Irr12.5L	−0.0076	−0.0057	29
Day_6Irr25L	−0.0062	−0.0051	19
Night_6Irr1.25L	−0.0117	−0.0092	25
Night_6Irr2.5L	−0.0108	−0.0090	18
Night_6Irr3.75L	−0.0104	−0.0084	21
Night_6Irr5L	−0.0099	−0.0079	23
Night_6Irr7.5L	−0.0091	−0.0071	24
Night_6Irr10L	−0.0084	−0.0066	25
Night_6Irr12.5L	−0.0079	−0.0062	25
Night_6Irr25L	−0.0059	−0.0048	22

$\Delta\%Ef_{res} - Ef_{nores}$ is the % difference.

diurnal average temperature of 34 ◦ C (heat health threshold), for the three hottest days of the heatwave (January 28–30). On the January 30 (diurnal mean = 35 ◦ C, Fig. 4), the model suggests a small amount of irrigation (e.g. 24Irr5L) was enough to lower most of the domain below the health threshold. However, on 28 and 29 January, conditions were extremely hot (diurnal mean = 38 ◦ C, Fig. 4) in Mawson Lakes. On these severe heat days, even with extensive irrigation (24Irr30L), much of the domain exceeded the heat health threshold (Fig. 12). Residential areas were particularly susceptible, with 80% and 60% of residential areas exceeding the heat health threshold on Julian day 28 and 29, respectively (Fig. 12).

Irrigation probably cannot protect residential areas against the most severe heatwave days. On severe heatwave days (e.g. 28 and 29 January) no volume of irrigation (unless impervious surfaces are irrigated) would cool residential areas below 34 ◦ C. This indicates a need for multiple approaches to mitigate excessive heat exposure, such as cool roofs, trees, and other green infrastructure. In addition to this, pavement watering, which is very uncommon in Australia, should be considered as heat mitigation strategy in more built-up areas (Daniel et al., 2016).

Nevertheless, irrigation modelling indicates that modest amount of irrigation could be used to provide valuable and feasible cooling during a heatwave event. While all pervious surfaces were irrigated in this study, in reality more focussed irrigation could be used, to provided targeted cooling benefits. For example, heavy irrigation (20 $L\,m^{-1}$) could be carried out in priority locations near age cared facilities and schools during a heatwave, thus providing cooling in vulnerable areas with a relatively small amount of total water used.

Threshold analysis illustrates the importance of understanding the full distribution of urban microclimate variability, rather than taking large-scale averages (e.g. 1 km). Larger scale averages of T_a may not provide useful information about the risk of human exposure to heat stress in a given area. Vulnerable populations (such as the elderly) may remain unprotected if they are residing in a microscale hotspot. Thus, practitioners should carefully identify T_a variability so that hotspots can be nullified and vulnerable populations protected. The high variability of T_a in urban areas highlights the challenges and opportunities of reducing human exposure to heat stress in urban environments.

3.3.2. Effects of irrigation on humidity and thermal comfort

While irrigation has been shown to significantly reduce T_a, the cooling effects of irrigation on outdoor human thermal comfort, could be offset by an increase in humidity. To explore this we calculated the humidex index (Masterton and Richardson, 1979) for each timestep across the domain. Humidex combines T_a and vapour pressure into a single index to reflect the perceived temperature (Humidex = T_a × 0.5555 × (vapour pressure −10). However, mean radiant temperature and wind speed significantly influence human thermal comfort. Thus, this calculation represents the effects of humidity on thermal comfort assuming constant wind speed and mean radiant temperature. Our results show that the average 3 pm humidex index decreased from 36.9 without irrigation ('some discomfort') to 34.6 for 24Irr20L ('some discomfort'). The background humidity was so low that the average increase in vapour pressure (0.5 hPa for 24Irr20L) did not negatively influence human thermal comfort during the heatwave. Humidex likely under-predicts the cooling benefits of thermal comfort, as it does not account for the reduction in mean radiant temperature associated with irrigation resulting from a reduction in daytime land surface temperature, which would further improve outdoor human thermal comfort during the day. Overall, these results suggest that irrigation will improve outdoor human thermal comfort during very hot and dry conditions.

3.4. Limitations and future research

The model was validated in this study, and as noted, was skilful enough to broadly capture the inter-urban diurnal microscale T_a variability. However, the model was validated during typical summertime conditions and recent research suggests SURFEX

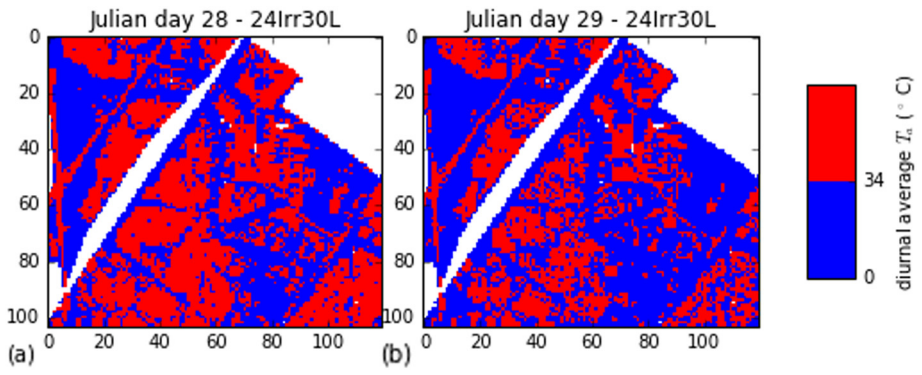

Fig. 12. The average diurnal T_a on for 24Irr30L on (a) Julian day 28 and (b) Julian day 29. Blue indicates diurnal average ≤34°C and red indicates diurnal average > 34°C.

can underestimate urban heat island intensity during heatwaves conditions (Hamdi et al., 2016). As such, for the heatwave simulations, T_a in urban areas may have been under-predicted in this study. As we do not have observational data from Mawson Lakes for heatwave conditions we cannot check the model performance during extreme heat.

Another significant limitation of this modelling analysis is the offline approach used. As no atmospheric model was used there were no horizontal interactions between the grid cells and no advection could occur. This means the modelling approach did not capture the larger scale mixing of heat in the atmosphere or any local-scale effects that contribute to T_a variability. Despite these limitations, the model was able to adequately capture most aspects of the intra-suburban T_a variability using land cover inputs from the surface directly adjacent (25 m). However, it must be acknowledged this approach does not capture all of the processes that influence microscale T_a in urban areas, and a comparison with an online simulation would be valuable. Given there is a need to understand microclimate variability for thermal comfort and heat stress reasons, the lack of appropriate modelling tools that can be used at the microscale is of concern. Urban planners are likely to want to model at this scale to understand exposure to heat stress variability. Therefore, if future urban planners want to assess the benefits of mitigation measures, for different urban layouts, then a microscale model (without the current limitations) would be helpful.

In addition to the lack of advection, Krayenhoff and Voogt (2010) noted differences in model sensitivity to surface energy balance changes for coupled and offline simulations (TEB). The authors note that for offline simulations of albedo measures, the atmosphere heats up as though no surface energy balance modifications have occurred. A similar effect in out study lead to an over-prediction of the latent heat flux. A lack of feedback with the atmosphere likely caused an exaggeration of the latent heat flux, because the very hot and dry atmospheric forcing data created a strong gradient for ET to occur. If the entire domain was irrigated (as in our simulations) this would cause both cooling and an increase in moisture in the urban boundary layer, meaning suburb scale irrigation effects must be carefully interpreted. However, in reality, it is more likely that pockets of localised irrigation will occur, and this is unlikely to cause significant feedback with the urban boundary layer, and thus the cooling predicted in our study is valid for localised irrigation cases.

Another limitation of this approach is the simplistic representation of the soil column in TEB-Veg. For example, currently there is no representation of sideways infiltration of moisture in the soil column. Given the importance of soil moisture in these simulations, we acknowledge this limitation could be a non-negligible source of error. However, despite TEB-Veg's limitations, the representation of the water cycle in TEB-Veg is more sophisticated than most other urban energy balance models. Another limitation was the generic parameters for urban surfaces used in this analysis. Grimmond et al. (2011), in Phase 2 of the International Urban Energy Balance Model Comparison (PILPS-urban), found the performance of most urban energy balance models deteriorated when building material information (radiative and thermal parameters) was provided; causing the authors to suggest that, given how difficult it is to gather appropriate values for material characteristics, their provision may not currently be worth the effort. Given the findings of PILPS-urban it is thought the use of generic urban parameters was justified. However, minimum diurnal T_a was over-predicted at most urban sites, suggesting the urban parameters used may have been incorrect or unreasonable. Generic natural parameters were also used and given the complex interactions between vegetation, soil, and irrigation, further refinement of site specific parameters (including LAI and stomatal resistance) is needed for future analyses. Further, the effects of different types of vegetation and/or soil on irrigation efficiency is likely to be variable, and therefore another important area for future research.

Lastly, this research did not directly consider the feasibility of the irrigation scenarios presented. This was a deliberate component of the research design, as we were interested in a systematic analysis of the cooling effects of irrigation on microclimate across different environments and microclimates. Despite this, water supply is important issue for irrigation. For example, due to the hot and dry conditions during and prior to the heatwave, there may not have been much stormwater available for irrigation. Mawson Lakes does have a sophisticated water re-use system, including stormwater harvesting and recycled water options, meaning availability of water for irrigation during the heatwave may have been high. Nevertheless, future research will directly consider the availability of different sources of water (stormwater, greywater, and potable water) during the heatwave case study, and how much cooling could have been achieved with that volume of water.

4. Conclusions

This study presents results from a range of simulations investigating the effect of irrigation on suburban T_a during heatwave conditions. The potential for irrigation to be used as cooling measure was explored and the SURFEX model was validated against high resolution in situ observational data. The main findings from the various simulations are as follows:

- **Offline surface energy balance modelling at high resolution was able to broadly capture diurnal average microscale T_a variability within the suburb, but the daily minima and maxima were not captured.** As such, the SURFEX scheme was not able to completely capture the microscale T_a variability in the Mawson Lakes suburb. A key message emerging from this research is urban microclimate is highly spatially variable. It is critical for human heat stress research that microclimate variability is captured. Lower resolution modelling may accurately simulate the average T_a of a suburb (or urban area), but such approaches will not capture the microscale variability within the domain. Ongoing research is needed so microscale variability can be well captured by urban surface energy balance models.

- **Irrigation can significantly reduce microscale T_a during heatwave conditions. However, over a given threshold (20 L $m^{-2}d^{-1}$) irrigation rapidly becomes less effective at reducing T_a.** This research supports the findings of previous studies that irrigation can have a cooling effect on both night time and daytime urban T_a. The results showed that it is hypothetically possible to cool the daily average temperature by up to 2.31 ° C. However, given the limitations of the modelling approach and the lack of atmospheric mixing that was captured, these findings are only truly valid for an isolated patch of irrigation. We would expect the cooling benefits to be lower if a coupled atmospheric model was used. It was also found the relationship between irrigation and cooling was non-linear, and above an irrigation rate of 20 L m^{-2} d^{-1} the thermal benefits of watering rapidly diminish during heatwave conditions. Further, the humidex index suggests that irrigation does improve human thermal comfort; increased humidity associated with irrigation does not offset the T_a cooling benefits. These results can be used to inform practitioners on how water should be used to achieve a desired amount of cooling during heatwave conditions. The magnitude of daily cooling at residential areas was lower than the domain average cooling, meaning irrigation can provide more cooling in highly pervious areas than in residential areas. Additionally, vegetation and soil type are likely to influence the effectiveness of irrigation cooling, and this is a key area for future research.
- **There is the potential to optimise the timing and volume of irrigation for thermal benefits.** Previous research has not considered the effect of the timing of irrigation on urban microclimate. The results from our analysis show the timing of irrigation does have an effect on average daily T_a cooling. Night time irrigation was more effective at reducing average daily T_a at irrigation rates below 25 L m^{-2} d^{-1}, while above 25 L m^{-2} d^{-1} daytime irrigation began to become more effective. These results suggest the same volume of water when applied at different times can be used to achieve different cooling outcomes. Future research should further explore the optimisation of irrigation timing for thermal benefits.
- **Irrigation cooling efficiency was higher in residential areas, but the total pervious fraction limited the total magnitude of cooling.** Our results suggest that irrigation in residential areas provided more cumulative cooling per L of water than in non-residential areas. However, residential areas had less total pervious surfaces than non-residential areas, meaning they were more likely to be exposed to extreme heat conditions (above heat health threshold) on very hot days. Although irrigation can provide useful cooling in residential areas, additional cooling measures are needed to protect vulnerable populations on severe heat days.
- **In the context of IUWM there is a good case for using irrigation as an heat mitigation measure during heatwaves.** IUWM seeks to reduce urban runoff and retain more water in urban areas for fit-for-purpose uses. This has positive benefits for urban ecology and flood mitigation. Therefore, reducing stormwater and greywater discharge into urban waterways is something that arguably should be done regardless of the thermal benefits. IUWM systems can be used to capture, treat, and store stormwater and greywater supplies. This water can then be re-integrated during heatwave conditions to provide the significant cooling benefits in the areas that most require cooling. As such, irrigation through stormwater reintegration can be used to simultaneously achieve thermal and hydrological sustainability benefits. Additionally, unlike other heat mitigation measures, irrigation provides cooling without permanently modifying the urban land surface. This means there are no potential negative cooling effects associated with irrigation during winter. With IUWM implemented, irrigation is a highly feasible cooling measure with notable advantages over other heat mitigation approaches.

Acknowledgments

This paper arose from PhD research funded by the Cooperative Research Centre for Water Sensitive Cities. Nigel Tapper and Andrew Coutts are funded by the Cooperative Research Centre for Water Sensitive Cities. The contribution of Matthias Demuzere is funded by the Flemish regional government through a contract as a FWO (Fund for Scientific Research) post-doctoral research fellow. We are indebted to all those who assisted during the Mawson Lakes field campaign: Andrew Coutts, Darren Hocking, Emma White, Naim Daliri-Milani, Stephen Livesley, Margaret Loughnan, Nigel Tapper, and Jason Beringer. A sincere thank you to Valéry Masson and others at Meteo-France who assisted with SURFEX modelling. Finally, thank you to Aude Lemonsu and the two anonymous reviewers who provided valuable feedback and ideas.

Appendix A

The TEB it is typically used for neighbourhood scale (100–1000 m) simulations or a single urban canopy. In this study we ran the model on a 25 m grid, meaning most grid points roughly approximate to a single canyon. However, such a fine grid could produce invalid results if a grid cell contains a high proportion of road or roof. As such, we also tested model performance at a resolution of 100 m (the same setup as in Section 2.3.2) to ensure that 25 m simulations produced acceptable results (Fig. A1). Overall, we found that model performance was very similar for the 100 m grid, although locations directly adjacent water bodies (e.g. TA-$6_{[Wtr+Out]}$) performed better at 25 m. Overall, these simulations give us confidence that a 25 m resolution is appropriate for this domain.

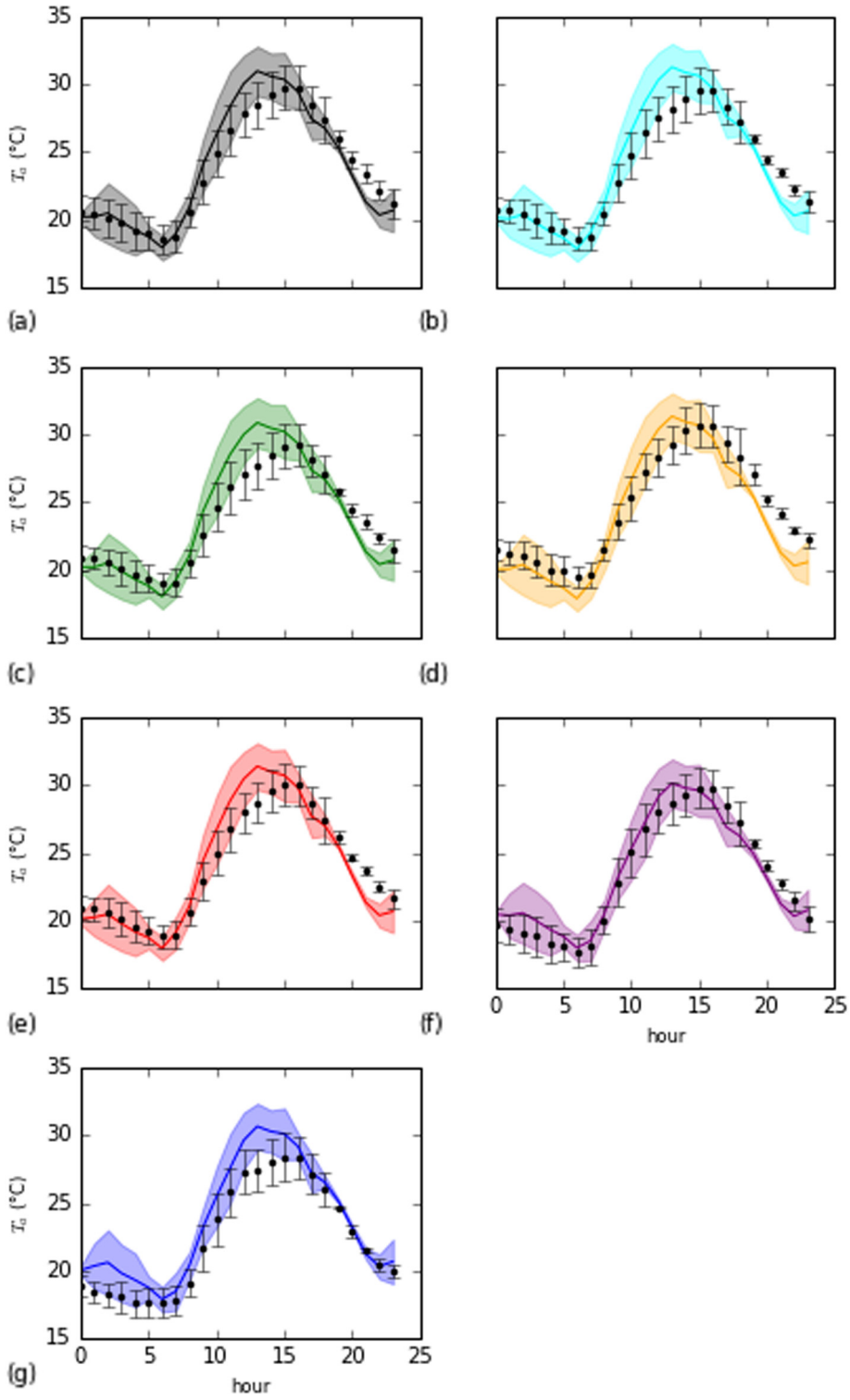

Fig. A1. The diurnal average modelled (lines) vs observed (bars) 2 m T_a during observational period (15 – 17 February), for a 100 m grid, grouped by T_a cluster: (a) all AWS sites, (b) TA-$1_{[Urb+Wtr]}$ (c) TA-$2_{[Mxd+Wtr]}$, (d) TA-$3_{[Urb+Mid]}$, (e) TA-$4_{[Urb+Res]}$, (f) TA-$5_{[Nat+Grs]}$, (g) TA-$6_{[Wtr+Out]}$ (see Fig. 3 for AWS clusters). Standard deviations are shown for both modelled and observed values.

Table A1
The statistical validation of SURFEX for AWS clusters in Mawson Lakes.

Cluster	*n*	*r*	*RMSE*	$T_{a[o]}$ (daily)	$T_{a[m]}$ (daily)	$T_{a[o]}$ (max)	$T_{a[m]}$ (max)	$T_{a[o]}$ (min)	$T_{a[m]}$ (min)
TA-$1_{[Urb+Wtr]}$	330	0.95	1.7	23.7 ± 4.0	24.0 ± 4.9	29.7	31.7	18.5	17.7
TA-$2_{[Mxd+Wtr]}$	264	0.94	1.8	23.6 ± 3.8	23.9 ± 4.7	29.4	31.2	18.9	17.9
TA-$3_{[Urb+Mid]}$	198	0.94	1.8	24.5 ± 4.1	24.0 ± 4.9	30.9	31.7	19.4	17.7
TA-$4_{[Urb+Res]}$	528	0.95	1.6	24.0 ± 4.1	24.1 ± 4.9	30.2	31.7	18.7	17.8
TA-$5_{[Nat+Grs]}$	396	0.94	1.6	23.3 ± 4.6	23.5 ± 4.4	29.9	30.6	17.4	17.7
TA-$6_{[Wtr+Out]}$	66	0.96	1.9	22.4 ± 4.3	23.7 ± 4.6	28.5	31.1	17.5	17.7
All	1782	0.94	1.7	23.7 ± 4.2	23.9 ± 4.8	29.9	31.4	18.4	17.8

$T_{a[o]}$ = mean observed air temperature.
$T_{a[m]}$ = mean modelled air temperature.
r = correlation coefficient.
RMSE = root mean square error.

References

Bowler, D.E., Buyung-Ali, L., Knight, T.M., Pullin, A.S., 2010. Urban greening to cool towns and cities: a systematic review of the empirical evidence. Landsc. Urban Plan. 97, 147–155.

Breuer, L., Eckhardt, K., Frede, H.-G., 2003. Plant parameter values for models in temperate climates. Ecol. Model. 169, 237–293.

Champeaux, J.L., Masson, V., Chauvin, F., 2005. ECOCLIMAP: A global database of land surface parameters at 1 km resolution. Meteorol. Appl. 12, 29–32. http://dx.doi.org/10.1017/S1350482705001519.

Clark, J.R., Kjelgren, R., et al. 1990. Water as a limiting factor in the development of urban trees. J. Arboric. 16, 203–208.

Coutts, A.M., Beringer, J., Tapper, N.J., 2007. Impact of increasing urban density on local climate: spatial and temporal variations in the surface energy balance in Melbourne, Australia. J. Appl. Meteorol. Climatol. 46, 477–493.

Coutts, A.M., Tapper, N.J., Beringer, J., Loughnan, M., Demuzere, M., 2012. Watering our cities: the capacity for water sensitive urban design to support urban cooling and improve human thermal comfort in the Australian context. Prog. Phys. Geogr. 36, 1–27.

Daniel, M., Lemonsu, A., Viguié, V., 2016. Role of watering practices in large-scale urban planning strategies to face the heat-wave risk in future climate. Urban Climate http://linkinghub.elsevier.com/retrieve/pii/S2212095516300505. http://dx.doi.org/10.1016/j.uclim.2016.11.001.

de Munck, C., 2013. Modélisation de la végétation urbaine et stratégies d'adaptation pour l'amélioration du confort climatique et de la demande énergétique en ville. http://ethesis.inp-toulouse.fr/archive/00002485/.

Demuzere, M., Coutts, A., Göhler, M., Broadbent, A., Wouters, H., van Lipzig, N., Gebert, L., 2014. The implementation of biofiltration systems, rainwater tanks and urban irrigation in a single-layer urban canopy model. Urban Climate 10, 148–170. http://dx.doi.org/10.1016/j.uclim.2014.10.012.

Gober, P., Brazel, A.J., Quay, R., Myint, S., Grossman-Clarke, S., Miller, A., Rossi, S., 2010. Using watered landscapes to manipulate urban heat island effects. J. Am. Plann. Assoc. 76, 109–121.

Grimmond, C.S.B., 1988. An evaporatranspiration-interception model for urban areas. Ph.D. thesis. University of British Columbia.,

Grimmond, C.S.B., Blackett, M., Best, M.J., Baik, J.J., Belcher, S.E., Beringer, J., Bohnenstengel, S.I., Calmet, I., Chen, F., Coutts, A., Dandou, A., Fortuniak, K., Gouvea, M.L., Hamdi, R., Hendry, M., Kanda, M., Kawai, T., Kawamoto, Y., Kondo, H., Krayenhoff, E.S., Lee, S.-H., Loridan, T., Martilli, A., Masson, V., Miao, S., Oleson, K., Ooka, R., Pigeon, G., Porson, A., Ryu, Y.H., Salamanca, F., Steeneveld, G.J., Tombrou, M., Voogt, J.A., Young, D.T., Zhang, N., 2011. Initial results from Phase 2 of the international urban energy balance model comparison. Int. J. Climatol. 31, 244–272.

Grimmond, C.S.B., Blacket, M., Barlow, J., Best, M.J., Baik, J.J., Belcher, S.E., Bohnenstengel, S.I., Calmet, I., Dandou, F.C., Fortuniak, K., Gouvea, M.L., Hamdi, R., Hendry, M., Kawai, T., Kawamoto, Y., Kondo, H., Krayenhoff, E.S., Lee, S.H., Loridan, T., Martilli, A., Masson, V., Miao, S., Oleson, K., Pigeon, G., Porson, A., Ryu, Y.H., Salamanca, F., Shashua-Bar, L., Steeneveld, G.J., Tombrou, M., Voogt, J., Young, D., Zhang, N., 2010. The international urban energy balance models comparison project: first results from phase 1. J. Appl. Meteorol. Climatol. 49, 1268–1292.

Grimmond, C.S.B., Oke, T.R., 1995. Comparison of heat fluxes from summertime observations in the suburbs of four North American cities. J. Appl. Meteorol. 34, 873–889.

Grimmond, C.S.B., Oke, T.R., 2002. Turbulent heat fluxes in urban areas: observations and a local-scale urban meteorological parameterization scheme (LUMPS). J. Appl. Meteorol. 41, 792–810.

Grossman-Clarke, S., Zehnder, J.A., Loridan, T., Grimmond, C.S.B., 2010. Contribution of land use changes to near-surface air temperatures during recent summer extreme heat events in the Phoenix Metropolitan Area. J. Appl. Meteorol. Climatol. 49, 1649–1664.

Hamdi, R., Duchêne, F., Berckmans, J., Delcloo, A., Vanpoucke, C., Termonia, P., 2016. Evolution of urban heat wave intensity for the Brussels capital region in the ARPEGE-climat a1b scenario. Urban Climate 17, 176–195. http://dx.doi.org/10.1016/j.uclim.2016.08.001.

Hamdi, R., Masson, V., 2008. Inclusion of a drag approach in the town energy balance (TEB) scheme: offline 1d evaluation in a street canyon. J. Appl. Meteorol. Climatol. 47, 2627–2644. http://dx.doi.org/10.1175/2008JAMC1865.1.

House-Peters, L.A., Chang, H., 2011. Modeling the impact of land use and climate change neighborhood-scale evaporation and nighttime cooling: a surface energy balance approach. Landsc. Urban Plan. 103, 139–155.

Kalanda, B.D., Oke, T.R., Spittlehouse, D.L., 1980. Suburban energy balance estimates for Vancouver, B.C., using the Bowen ratio-energy balance approach. J. Appl. Meteorol. 19, 791–802.

Kawai, T., Kanda, M., Kawai, T., Kanda, M., 2010. Urban energy balance obtained from the comprehensive outdoor scale model experiment. Part I: basic features of the surface energy balance. J. Appl. Meteorol. Climatol. 49, 1341–1359. http://dx.doi.org/10.1175/2010JAMC1992.1.

Kawai, T., Kanda, M., Narita, K., Hagishima, A., 2007. Validation of a numerical model for urban energy-exchange using outdoor scale-model measurements. Int. J. Climatol. 27, 1931–1942. http://dx.doi.org/10.1002/joc.1624.

Konarska, J., Uddling, J., Holmer, B., Lutz, M., Lindberg, F., Pleijel, H., Thorsson, S., 2016. Transpiration of urban trees and its cooling effect in a high latitude city. Int. J. Biometeorol. 60, 159–172.

Krayenhoff, E.S., Voogt, J.A., 2010. Impacts of urban albedo increase on local air temperature at daily-annual time scales: model results and synthesis of previous work. J. Appl. Meteorol. Climatol. 49, 1634–1648.

Lemonsu, A., Grimmond, C.S.B., Masson, V., 2004. Modeling the surface energy balance of the core of an old Mediterranean city: Marseille. J. Appl. Meteorol. 43, 312–327.

Lemonsu, A., Kounkou-Arnaud, R., Desplat, J., Salagnac, J.-L., Masson, V., 2012a. Evolution of the Parisian urban climate under a global changing climate. Clim. Change 116, 679–692.

Lemonsu, A., Masson, V., Shashua-Bar, L., Erell, E., Pearlmutter, D., 2012, nov. Inclusion of vegetation in the town energy balance model for modelling urban green areas. Geosci. Model Dev. 5, 1377–1393. http://www.geosci-model-dev.net/5/1377/2012/gmd-5-1377-2012.html. http://dx.doi.org/10.5194/gmd-5-1377-2012.

Loughnan, M., Tapper, N., Phan, T., Lynch, K., McInnes, J.A., 2013. A spatial vulnerability analysis of urban populations during extreme heat events in Australian capital cities. Technical Report National Climate Change Adaptation Research Facility Gold Coast. http://www.nccarf.edu.au/publications/spatial-vulnerability-urban-extreme-heat-events.

Masson, V., 2000. A physically-based scheme for the urban energy budget in atmospheric models. Boundary Layer Meteorol. 94, 357–397.

Masson, V., Grimmond, C.S.B., Oke, T.R., 2002. Evaluation of the Town Energy Balance (TEB) scheme with direct measurements from dry districts in two cities. J. Appl. Meteorol. 41, 1011–1026.

Masson, V., Le Moigne, P., Martin, E., Faroux, S., Alias, A., Alkama, R., Belamari, S., Barbu, A., Boone, A., Bouyssel, F., Brousseau, P., Brun, E., Calvet, J.-C., Carrer, D., Decharme, B., Delire, C., Donier, S., Essaouini, K., Gibelin, A.-L., Giordani, H., Habets, F., Jidane, M., Kerdraon, G., Kourzeneva, E., Lafaysse, M., Lafont, S., Lebeaupin Brossier, C., Lemonsu, A., Mahfouf, J.-F., Marguinaud, P., Mokhtari, M., Morin, S., Pigeon, G., Salgado, R., Seity, Y., Taillefer, F., Tanguy, G., Tulet, P., Vincendon, B., Vionnet, V., Voldoire, A., 2013. The SURFEXv7.2 land and ocean surface platform for coupled or offline simulation of earth surface variables and fluxes. Geosci. Model Dev. 6, 929–960. http://www.geosci-model-dev.net/6/929/2013/gmd-6-929-2013.html. http://dx.doi.org/10.5194/gmd-6-929-2013.

Masson, V., Seity, Y., 2009. Including atmospheric layers in vegetation and urban offline surface schemes. J. Appl. Meteorol. Climatol. 48, 1377–1397. http://dx.doi.org/10.1175/2009JAMC1866.1.

Masterton, J., Richardson, F., 1979. Humidex: A Method of Quantifying Human Discomfort due to Excessive Heat and Humidity. Downsview, Ont.: Atmospheric Environment.

Mitchell, V.G., Cleugh, H.A., Grimmond, C.S.B., Xu, J., 2008. Linking urban water balance and energy balance models to analyse urban design options. Hydrol. Process. 22, 2891–2900. http://dx.doi.org/10.1002/hyp.6868.

National Climate Centre, 2009. Special climate statement 17, the exceptional January-February 2009 heatwave in south-eastern Australia. Technical Report Bureau of Meteorology. http://www.bom.gov.au/climate/current/statements/scs17c.pdf.

Oke, T., 1987. Boundary Layer Climates. Methuen, London.

Oke, T.R., Crowther, J.M., McNaughton, K.G., Monteith, J.L., Gardiner, B., 1989. The micrometeorology of the urban forest [and discussion]. Philos. Trans. R. Soc., B 324, 335–349. http://rstb.royalsocietypublishing.org/content/324/1223/335. http://dx.doi.org/10.1098/rstb.1989.0051.

Oke, T.R., McCaughey, J.H., 1983. Suburban-rural energy balance comparisons for Vancouver, B.C.: an extreme case? Boundary Layer Meteorol. 26, 337–354.

Roberts, S.M., Oke, T.R., Grimmond, C., Voogt, J.A., 2006. Comparison of four methods to estimate urban heat storage. J. Appl. Meteorol. Climatol. 45, 1766–1781.

Stewart, I.D., Oke, T.R., 2012. Local climate zones for urban temperature studies. Bull. Am. Meteorol. Soc. 93, 1879–1900. http://dx.doi.org/10.1175/BAMS-D-11-00019.1.

Walsh, C.J., Fletcher, T.D., Ladson, A.R., 2005. Stream restoration in urban catchments through redesigning stormwater systems: looking to the catchment to save the stream. J. N. Am. Benthol. Soc. 24, 690–705. http://dx.doi.org/10.1899/04-020.1.

Ward, J.H.J., 1963. Hierarchical grouping to optimize an objective function. J. Am. Stat. Assoc. 58, 236–244. http://www.jstor.org/discover/2282967?sid=21105652729063&uid=4&uid=2&uid=2134&uid=3737536&uid=70.

Wouters, H., Demuzere, M., De Ridder, K., van Lipzig, N., 2015. The Impact of Impervious Water-Storage Parametrization on Urban Climate Modelling. EGU General Assembly 2015, held 12-17 April, 2015 in Vienna, Austria. id.9483, 17.

Zhu, S., Guan, H., Bennett, J., Clay, R., Ewenz, C., Benger, S., Maghrabi, A., Millington, A.C., 2013. Influence of sky temperature distribution on sky view factor and its applications in urban heat island. Int. J. Climatol. 1837–1843. http://dx.doi.org/10.1002/joc.3660.